BELLCOMM, INC.
955 L'ENFANT PLAZA NORTH, S.W., WASHINGTON, D.C. 20024

COVER SHEET FOR TECHNICAL MEMORANDUM

TITLE- An Analysis of Apollo 10 Tracking Data Utilizing the POLAR Version of the Osculating Lunar Elements Program

TM- 69-2014-9

DATE- September 30, 1969

FILING CASE NO(S)- 310

AUTHOR(S)- M. V. Bullock
A. J. Ferrari

FILING SUBJECT(S)
(ASSIGNED BY AUTHOR(S))- Orbit Determination

ABSTRACT

An analysis of twenty-four front side passes (after the LOI-2 trajectory circularization maneuver) of Apollo 10 CSM Doppler data was made using a version of the Osculating Lunar Elements Program which eliminates singularities of near equatorial, circular orbits. Solutions were obtained on a two pass regression zone/two pass propagation zone basis.

The quality of the Apollo 10 data used in this analysis is of three types: free flight data, data containing attitude maneuvers and waste water dumps, and data containing CSM maneuvers. Solutions obtained from the free flight data manifested a growth in Doppler errors of a factor of two from regression zone to propagation zone. Those obtained from data containing attitude maneuvers and waste water dumps possessed a growth factor of five. Those solutions obtained from data containing the CSM separation and evasive maneuvers resulted in extremely large propagation zone Doppler errors.

A local vertical comparison of five different propagated solutions and their corresponding local regression zone solutions showed large dispersions in the cross track component. Attitude maneuvers present in three of the comparisons resulted in large radial and down range errors. Comparisons made on the remaining two cases (free flight data) led to 50 - 90% smaller radial and down range errors. The presence of the large plane dispersions could be due to either the existence of attitude maneuvers in the data or the lack of sensitivity of the Doppler data to planar information.

In summary, it is felt that the POLAR program can do orbital estimation to sufficient accuracy for the Lunar Exploration Program LM landing requirements in the radial and down range directions if the computer program's assumption of no propulsion during the periods involved is fulfilled by the spacecraft. Even small thrusting, of magnitudes not normally measured by the spacecraft or reported to the MCC-H, will reduce this accuracy markedly. Out-of-plane, POLAR produces accuracy equal to or better than current MCC-H RTCC methods, but still a factor of 3 or 4 worse than required and unpredictably random.

DISTRIBUTION

COMPLETE MEMORANDUM TO

CORRESPONDENCE FILES:

OFFICIAL FILE COPY
plus one white copy for each additional case referenced

TECHNICAL LIBRARY (4)

NASA Headquarters

C. M. Lee/MA
T. A. Keegan/MA-2
R. A. Petrone/MA

Goddard Space Flight Center

J. Barsky/554

Langley Research Center

W. H. Michael, Jr./152A
R. H. Tolson/152A

Manned Spacecraft Center

M. Grogan/FM4
J. P. Mayer/FM
J. C. McPherson/FM4
E. Schiesser/FM4
W. Wollenhaupt/FM4

Bell Telephone Laboratory

W. M. Boyce/MH

Jet Propulsion Laboratory

P. Gottlieb/233-307
J. Lorell/156-217
P. Muller/198-112A
W. L. Sjogren/180-304

MIT

R. H. Battin

COMPLETE MEMORANDUM TO (CONT'D)

Bellcomm, Inc.

D. R. Anselmo
A. P. Boysen, Jr.
J. O. Cappellari, Jr.
D. A. Corey
W. W. Ennis
D. R. Hagner
W. G. Heffron
T. B. Hoekstra
B. T. Howard
D. B. James
S. L. Levie, Jr.
M. Liwshitz
D. D. Lloyd
W. I. McLaughlin
J. Z. Menard
V. S. Mummert
B. G. Niedfeldt
D. H. Novak
R. V. Sperry
C. C. Tang
W. B. Thompson
J. W. Timko
J. E. Volonte
R. L. Wagner
M. P. Wilson
All Members of Department 2014
Department 1024 File

ABSTRACT ONLY TO

Bellcomm, Inc.

I. M. Ross

BELLCOMM, INC.
955 L'ENFANT PLAZA NORTH, S.W. WASHINGTON, D.C. 20024

SUBJECT: An Analysis of Apollo 10 Tracking Data Utilizing the POLAR Version of the Osculating Lunar Elements Program Case 310

DATE: September 30, 1969

FROM: M. V. Bullock
A. J. Ferrari

TM-69-2014-9

TECHNICAL MEMORANDUM

I. INTRODUCTION

During the Lunar Parking Orbit (L.P.O.) phase of the Apollo 10 mission (post LOI-2 circularization maneuver), twenty-eight front side passes of Command Service Module (CSM) Doppler tracking data were acquired by the Deep Space Network (DSN) and the Manned Space Flight Network (MSFN). An analysis of the first twenty-four passes of these data was made using the POLAR version of the Osculating Lunar Elements Program (O.L.E.P.). In order to maintain processing consistency between Real Time Computer Center results using the R2 lunar gravity field and those obtained from POLAR, these data were processed on a two pass regression zone and a two pass propagation zone basis. Post flight analysis of these data using POLAR is of special interest in light of the navigation problems encountered during the Apollo 11 lunar landing mission. This memorandum presents an analysis of the results obtained.

II. MATHEMATICAL FORMULATION

The basic concept of POLAR is the representation of some of the low-eccentricity orbital elements, a, $e_c = e \cos \omega$, $e_s = e \sin \omega$, Ω, I, $m = M + \omega$, by linearly time-varying functions. In order to avoid the numerical singularities associated with near equatorial orbits, the low-eccentricity elements are defined in a pseudo selenocentric coordinate frame ($\bar{X}'$) which represents a truly equatorial orbit as a polar orbit. This transformation is accomplished by rotating the initial estimate of the selenocentric state at epoch ($\bar{X}$) through two of its associated Euler angles ($\hat{\Omega}$, $\hat{I}$) as follows:

$$[\bar{X}'] = [M]\ [\bar{X}]$$

and

$$[\dot{\bar{X}}'] = [M]\ [\dot{\bar{X}}] \qquad (1)$$

where:

$$[M] = \begin{bmatrix} \cos \hat{\Omega} & \sin \hat{\Omega} & 0 \\ -\sin \hat{\Omega} \cos (\hat{I} + 90) & \cos \hat{\Omega} \cos (\hat{I} + 90) & \sin (\hat{I} + 90) \\ \sin (\hat{I} + 90) \sin \hat{\Omega} & -\sin (\hat{I} + 90) \cos \hat{\Omega} & \cos (\hat{I} + 90) \end{bmatrix}$$

Since the original estimates for $\hat{\Omega}$ and $\hat{I}$ are close to their converged values, it is only necessary to make this transformation once prior to beginning the orbit determination process; i.e., $\hat{\Omega}$ and $\hat{I}$ are constants.

During the data reduction or orbit determination, estimates are obtained for both the six low-eccentricity elements and some of their corresponding linear time dependent terms. The actual data reduction is accomplished using a classical least squares algorithm which minimizes the error squared or residual obtained from processing k observations by differentially correcting the n solution parameters $\{\alpha_i\}$ as follows:

$$\Delta\alpha_i = \left[\sum_{i=1}^{k} J^T (t_i) W (t_i) J (t_i) \right]^{-1} \sum_{i=1}^{k} J^T (t_i) W (t_i) \Delta\lambda (t_i) \quad (2)$$

where: $\Delta\lambda (t_i) = \lambda (t_i) - \hat{\lambda} (t_i)$

In this expression $\Delta\alpha_i$ is the differential correction vector (n X 1), J (t_i) is a row vector (1 X n) containing the partial derivatives of the observable with respect to the parameters which are to be estimated (evaluated at time t_i), J^T is the transpose of the J vector, W (t_i) is the weighting matrix (1 X 1), λ (t_i) is the t_i^{th} Doppler observation, and $\hat{\lambda}$ (t_i) is the estimated observable at time t_i.

A typical entry to either the J or J^T vector (consider the case of Ω (t) = $\Omega_o + \Omega_1$ t) is given by the chain rule for differentiable functions as follows:

$$\left.\frac{\partial\hat{\lambda}}{\partial\Omega_1}\right|_{t_i} = \sum_{i=1}^{3}\sum_{j=1}^{3}\left[\frac{\partial\hat{\lambda}}{\partial X_i}\frac{\partial X_i}{\partial X'_j}\frac{\partial X'_j}{\partial\Omega}\frac{\partial\Omega}{\partial\Omega_1} + \frac{\partial\hat{\lambda}}{\partial\dot{X}_i}\frac{\partial\dot{X}_i}{\partial\dot{X}'_j}\frac{\partial\dot{X}'_j}{\partial\Omega}\frac{\partial\Omega}{\partial\Omega_1}\right]_{t_i} \quad (3)$$

In this expression $\frac{\partial\hat{\lambda}}{\partial X_i}$ and $\frac{\partial\hat{\lambda}}{\partial\dot{X}_i}$ are the partial derivatives of the observable with respect to the selenocentric position and velocity respectively, $\frac{\partial X_i}{\partial X'_j}$ and $\frac{\partial\dot{X}_i}{\partial\dot{X}'_j}$ are partial derivatives of selenocentric position and velocity with respect to the pseudo selenocentric position and velocity, $\frac{\partial X'_j}{\partial\Omega}$ and $\frac{\partial\dot{X}'_j}{\partial\Omega}$ the partial derivatives of the pseudo selenocentric position and velocity with respect to the particular orbital element in question (longitude of the ascending node in this case), $\frac{\partial\Omega}{\partial\Omega_1}$ is the partial derivative of the orbital element with respect to the parameter to be estimated. Each partial derivative appearing in equation (3) is evaluated at some time t_i.

The first step in formulating the estimated observable, $\hat{\lambda}$ (t_i), is to evaluate the low-eccentricity elements at time t_i. The resulting orbital state is then converted to

the pseudo selenocentric state, $\bar{X}'$ and $\dot{\bar{X}}'$, using the classical orbital to state equations.[1] The pseudo selenocentric state is transformed into the selenocentric state as follows:

$$\left.\begin{aligned} [\bar{X}] &= [M]^{-1} [\bar{X}'] \\ [\dot{\bar{X}}] &= [M]^{-1} [\dot{\bar{X}}'] \end{aligned}\right\} \tag{4}$$

The vehicle position and velocity in selenocentric coordinates can be transformed to earth-referenced topocentric coordinates, $\bar{X}''$, as follows:

$$\left.\begin{aligned} \bar{X}'' &= \bar{X} + \bar{X}_e - \bar{X}_s \\ \dot{\bar{X}}'' &= \dot{\bar{X}} + \dot{\bar{X}}_e - \dot{\bar{X}}_s \end{aligned}\right\} \tag{5}$$

where $\bar{X}_e$ and $\dot{\bar{X}}_e$ are ephemeral position and velocity of the moon's center with respect to that of the earth, and $\bar{X}_s$ and $\dot{\bar{X}}_s$ are position and velocity of the tracking station. The estimated observable, $\hat{\lambda}$, can now be expressed in terms of the topocentric state of the vehicle as follows:

$$\hat{\lambda} = \hat{\lambda} \ (\bar{X}'', \ \dot{\bar{X}}'') \tag{6}$$

The processing of k Doppler observations and the resulting set of differential corrections $\{\Delta\alpha_i\}$ constitute one computing iteration. The convergence criterion for any two successive iterations is as follows:

---

1. Kaula, W. M., Theory of Satellite Geodesy, Blaisdell Publishing Company, Waltham, Massachusetts, pp. 23-24.

$$\left.\frac{\sum_{i=1}^{k}\left[\Delta\lambda\ (t_i)\right]^2}{\sum_{i=1}^{k}\left[\Delta\lambda\ (t_i)\right]^2}\right|_{(I)}^{(I-1)} - 1 < \delta \qquad (7)$$

where δ is a small positive number (10^{-4}) and (I-1) and (I) designate the (I-1) and (I) computing iterations.

The semi-major axis does not appear in POLAR as an explicit solution parameter. The estimate for the linear portion of the modified anomaly ($m\ (t) = m_o + m_1\ t$) is used to imply a corresponding semi-major axis by using the classical Kepler relationship:

$$m_1 = \sqrt{\frac{\mu}{a^3}} \qquad (8)$$

or:

$$a = \left[\sqrt{\frac{\mu}{m_1^2}}\right]^{\frac{1}{3}}$$

where μ is the Newtonian constant times the lunar mass.

III. ANALYSIS OF RESULTS

The vehicle state in lunar orbit (referenced to the pseudo selenocentric coordinate frame) is represented by a fundamental parameter set consisting of the following nine parameters:

$$e_c(t) = e_{co} + e_{c1}\, t$$

$$e_s(t) = e_{so} + e_{s1}\, t$$

$$\Omega(t) = \Omega_o + \Omega_1\, t$$

$$I(t) = I_o$$

$$m(t) = m_o + m_1\, t$$

Changes to the semi-major axis, from iteration to iteration, are made through the Kepler relationship given in equation (8). These parameters model the free flight trajectory of the vehicle in lunar orbit.

The free flight (absence of propulsive effects) quality of the Doppler tracking data acquired by the DSN and MSFN must be established prior to proceeding with the analysis. The Apollo 10 data utilized can be characterized as follows:

1. Data acquired from CSM free flight.
2. Data acquired during CSM water dumps and during coupled and uncoupled[1] maneuvers.
3. Data acquired during CSM ΔV Service Propulsion System (S.P.S.) burns.

The wast water dumps occurred at the end of pass Number 9 and between passes Number 25 and 96.[2] The coupled attitude maneuvers performed by the CSM took place during pass Numbers 4, 13, 24-27, and 30.[3] An uncoupled maneuver took place during pass Number 11. The CSM separation maneuver and

---

1. Maneuver results in CSM rotation and translation.

2. Apollo 10/AS-505 MSFN Metric Tracking Performance, Goddard Space Flight Center, Greenbelt, Maryland, May 1969, X-832-69-224, pp. 63-65.

3. Uncoupled attitude maneuvers could have also taken place during these passes if the quad fuel became unbalanced or if the crew used the minimum impulse hand controller.

the CSM evasive maneuvers took place during passes Number 12 and 17 respectively.[1] The processing of Apollo 10 data by both POLAR and the RTCC orbit determination program showed possible propulsive effects between passes Number 5 and 6 and during pass Number 23. A summary of these maneuvers and propulsive vents is given in Table I.

The two pass propagation zone errors obtained from the POLAR processing of Apollo 10 data are a direct function of the free flight quality of the Doppler. In each of the cases considered, when propulsive thrusts occurred in either the regression zone or the propagation zone, this naturally resulted in larger Doppler errors. The Doppler errors obtained from each two pass regression zone/two pass propagation zone are shown in Figures 1-22. These figures are presented to show the Doppler error growth characteristics for each of the solutions obtained.

a. Analysis of Free Flight Data

Of all the Apollo 10 data used in the analysis only four two pass regression zone (RZ)/two pass propagation zone (PZ) solutions, 6-7 → 8-9, 7-8 → 9-10, 18-19 → 20-21, and 19-20 → 21-22, (See Figures 4, 5, 16 and 17) show near free flight quality. (Pass Number 9 contains a water dump.) Each of these solutions is characterized by small regression zone errors (peak-to-peak about 0.8 fps) and small propagation zone errors (1.5 fps peak-to-peak or less). The 6-7 → 8-9 (Figure 4) solution is of particularly good quality and possesses the least growth in errors from RZ to PZ of all the data analyzed.

b. Analysis of Data Containing Attitude Maneuvers and Water Dumps

The solutions obtained for passes 3-4 → 5-6, 4-5 → 6-7, 5-6 → 7-8, 8-9 → 10-11, 13-14 → 15-16, 20-21 → 22-23, 21-22 → 23-24, 22-23 → 24-25, 23-24 → 25-26, and 24-25 → 26-27 (See Figures 1, 2, 3, 6, 11, 18, 19, 20, 21, and 22) contain either some CSM attitude maneuvers or water dumps in either the regression zone or the propagation zone. Again each of these solutions is characterized by small regression zone errors (about 0.8 fps peak-to-peak); however, in this case the propagation errors grow by about a factor of five over those of each regression zone (maximum peak-to-peak errors of about 5 fps). The presence of the attitude maneuvers in the Doppler data may be responsible for this large error growth rate.

c. Analysis of Data Containing CSM/SPS Maneuvers

The solutions obtained for passes 9-10 → 11-12, 10-11 → 12-13, 11-12 → 13-14, 12-13 → 14-15 (See Figures 7-10) and passes 14-15 → 16-17, 15-16 → 17-18, 16-17 → 18-19, 17-18 → 19-20 (See Fig. 12-15) contain the CSM separation (pass 12) and evasive maneuvers

1. Apollo 10/AS-505 MSFN Metric Tracking Performance, pp. 46-47.

(pass 17) respectively in either the regression or propagation zones. Each of these solutions possesses small regression zone errors (about 0.8 fps peak-to-peak). The propagation zone Doppler errors associated with each of these regression zones are extremely large since no ΔV has been modeled in the POLAR equations of motion. It is interesting to note that when each of these groups of passes is examined in conjunction with all the other solutions obtained, the effect of the CSM maneuvers becomes readily apparent. The occurrence of a maneuver in the first pass of a two pass regression zone is less critical than one in the second pass. (See Figures 10 and 15.)

A compilation of the statistical qualities (mean, standard deviation, and root sum of squares) of both the regression and propagation zone errors is given in Table II.

IV. LOCAL SOLUTION COMPARISON

In order to analyze the forward propagation characteristics of a two pass POLAR solution, a comparison was made in a local vertical coordinate frame (U-radial, V-down range, W-out of plane) among the several two pass propagation zone solutions and the corresponding two pass local solutions. In all cases the local solution was considered as the standard since it minimizes the residuals associated with the Doppler observable.

Comparisons were made among four pre-DOI solutions and one post DOI solution; 3-4 $\rightarrow \hat{5}\text{-}\hat{6}$ versus 5-6, 4-5 $\rightarrow \hat{6}\text{-}\hat{7}$ versus 6-7, 5-6 $\rightarrow \hat{7}\text{-}\hat{8}$ versus 7-8, 6-7 $\rightarrow \hat{8}\text{-}\hat{9}$ versus 8-9, 18-19 $\rightarrow \hat{20}\text{-}\hat{21}$ versus 20-21. ($\hat{}$ indicates propagation zone). The first three comparisons made involve passes which include attitude maneuvers in the regression zone.

The table below presents the maximum deviations (δU, δV, δW) obtained in local vertical coordinates for the five cases considered:

Passes:	$\lvert\delta U_{max}\rvert$ (feet)	$\lvert\delta V_{max}\rvert$ (feet)	$\lvert\delta W_{max}\rvert$ (feet)
$\hat{5}\text{-}\hat{6}$ vs. 5-6	1900	8650	2175
$\hat{6}\text{-}\hat{7}$ vs. 6-7	1100	4970	15,600
$\hat{7}\text{-}\hat{8}$ vs. 7-8	1800	10,000	23,500
$\hat{8}\text{-}\hat{9}$ vs. 8-9	215	875	6800
$\hat{20}\text{-}\hat{21}$ vs. 20-21	700	1700	9700

The effects of the attitude maneuvers can most clearly be seen in the radial and down range deviations obtained for the first three comparisons. In the last two cases both the radial and down range errors become smaller by 50 to 90%. In all cases considered (with the exception of the first), the out of plane errors obtained were extremely large. These errors may reflect the effects of the attitude maneuvers, or they may be a manifestation of the Doppler insensitivity to the planar elements (I and Ω).

V. CONCLUSIONS

Twenty four passes of CSM Doppler tracking data acquired by the MSFN and DSN were analyzed using POLAR on a two pass regression zone and two pass propagation zone basis. The fundamental parameter set used in the POLAR processing of Apollo 10 data consists of the following nine parameters: e_{so}, e_{s1}, e_{co}, e_{c1}, Ω_o, Ω_1, I_o, m_o, and m_1.

Solutions obtained on free flight Apollo 10 data possessed a growth in Doppler errors from the regression zone to propagation zone of a factor of two or less. The solutions from data containing either attitude maneuvers or waste water dumps manifested an error growth rate from regression zone to propagation zone of a factor of five. The solutions obtained from data containing the CSM separation and evasive maneuvers led to extremely large propagation errors.

A comparison of five POLAR propagated solutions with their respective local regression zones was made in local vertical coordinates. The attitude maneuvers present in three of the comparisons led to larger radial and down range errors. The comparisons made on the two remaining cases (free flight data) led to 50 to 90% smaller radial and down-range errors of the order of 500 and 1200 ft. respectively at the end of two passes of forward propagation. In four of the five cases considered large plane deviations were experienced. The presence of these plane inconsistencies could be due to the attitude maneuvers or the lack of sensitivity of the Doppler data to planar information (I,Ω).

In summary, it is felt that the POLAR program can do orbital estimation to sufficient accuracy for the Lunar Exploration Program LM landing requirements in the radial and down range directions if the computer program's assumption of no propulsion during the periods involved is fulfilled by the spacecraft. Even small thrusting, of magnitudes not normally measured by the spacecraft or reported to the MCC-H, will

reduce this accuracy markedly. Out-of-plane, POLAR produces accuracy equal to or better than current MCC-H RTCC methods, but still a factor of 3 or 4 worse than required and unpredictably random.

M. V. Bullock

M. V. Bullock

A. J. Ferrari

A. J. Ferrari

2014-$^{MVB}_{AJF}$-ksc

Attachments
Table I-II
Figures 1-22

TABLE I

Apollo 10 Maneuvers and Propulsive Thrusts

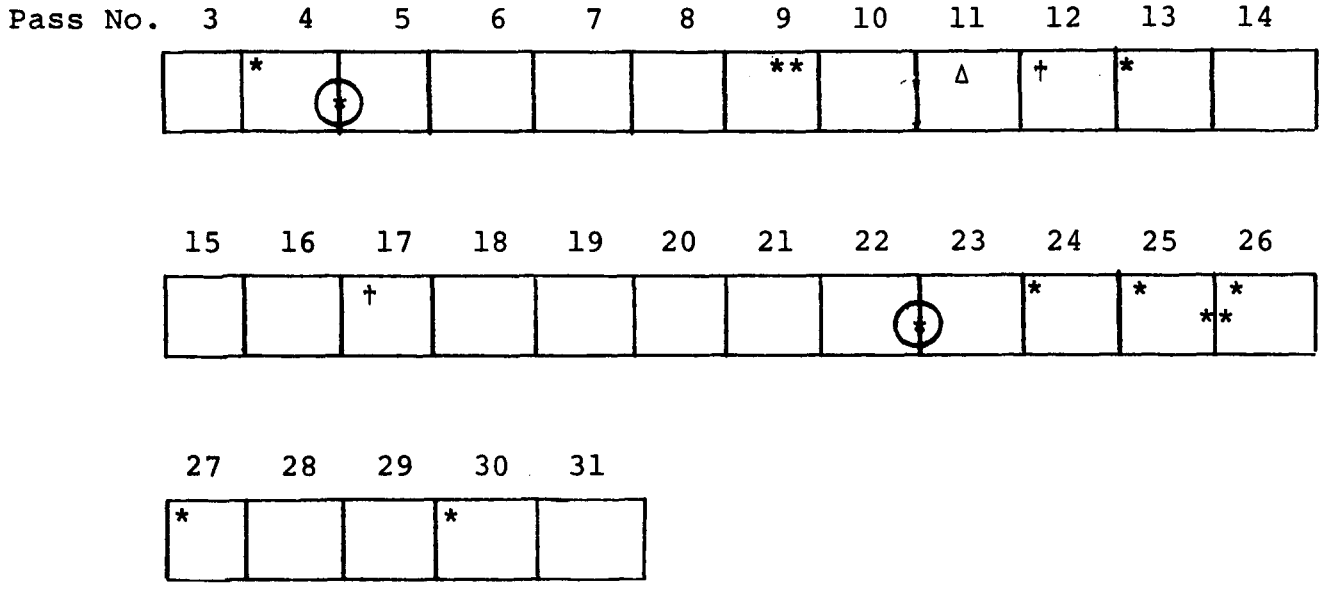

Δ	Uncoupled Maneuver
*	Coupled Maneuver
**	Water Dump
†	Powered Flight
⊛	Speculate Maneuver of Some Kind

TABLE II

Pass No.	Mean (fps)		Standard Deviation (fps)		Root Sum of Squares (fps)	
	R.Z.	P.Z.	R.Z.	P.Z.	R.Z.	P.Z.
3,4	.0110	-.9759	.1783	1.187	.1786	1.537
4,5	.0136	.2552	.1889	.7467	.1894	.7891
5,6	.0085	1.167	.1831	1.243	.1833	1.705
6,7	.0190	.0364	.1840	.2186	.1850	.2216
7,8	.0115	.1486	.1844	.3023	.1847	.3369
8,9	.0090	1.071	.1835	1.351	.1837	1.724
9,10	.0077	3.014	.1833	4.703	.1835	5.586
10,11	.0198	6.998	.1919	7.629	.1929	10.35
11,12	.0042	-.6894	.2113	3.407	.2114	3.476
12,13	.0266	-.7350	.1832	1.244	.1851	1.445
13,14	-.0012	-.1060	.1652	.8465	.1653	.8531
14,15	-.0004	-4.892	.1668	3.979	.1668	6.306
15,16	.0385	-14.47	.1900	19.68	.1938	24.43
16,17	.0134	-30.78	.3294	28.59	.3297	42.01
17,18	.0115	-.5630	.1797	.5898	.1801	.8154
18,19	.0009	-.2997	.1693	.3825	.1693	.4860
19,20	.0161	.3535	.1602	.3919	.1610	.5278
20,21	.0111	.7038	.1872	.8004	.1875	1.066
21,22	.0244	.4136	.1816	.8588	.1833	.9532
22,23	.0372	-1.571	.1927	2.082	.1963	2.608
23,24	.0191	-.5234	.1878	1.011	.1888	1.138
24,25	.0187	-1.059	.1917	1.174	.1926	1.581

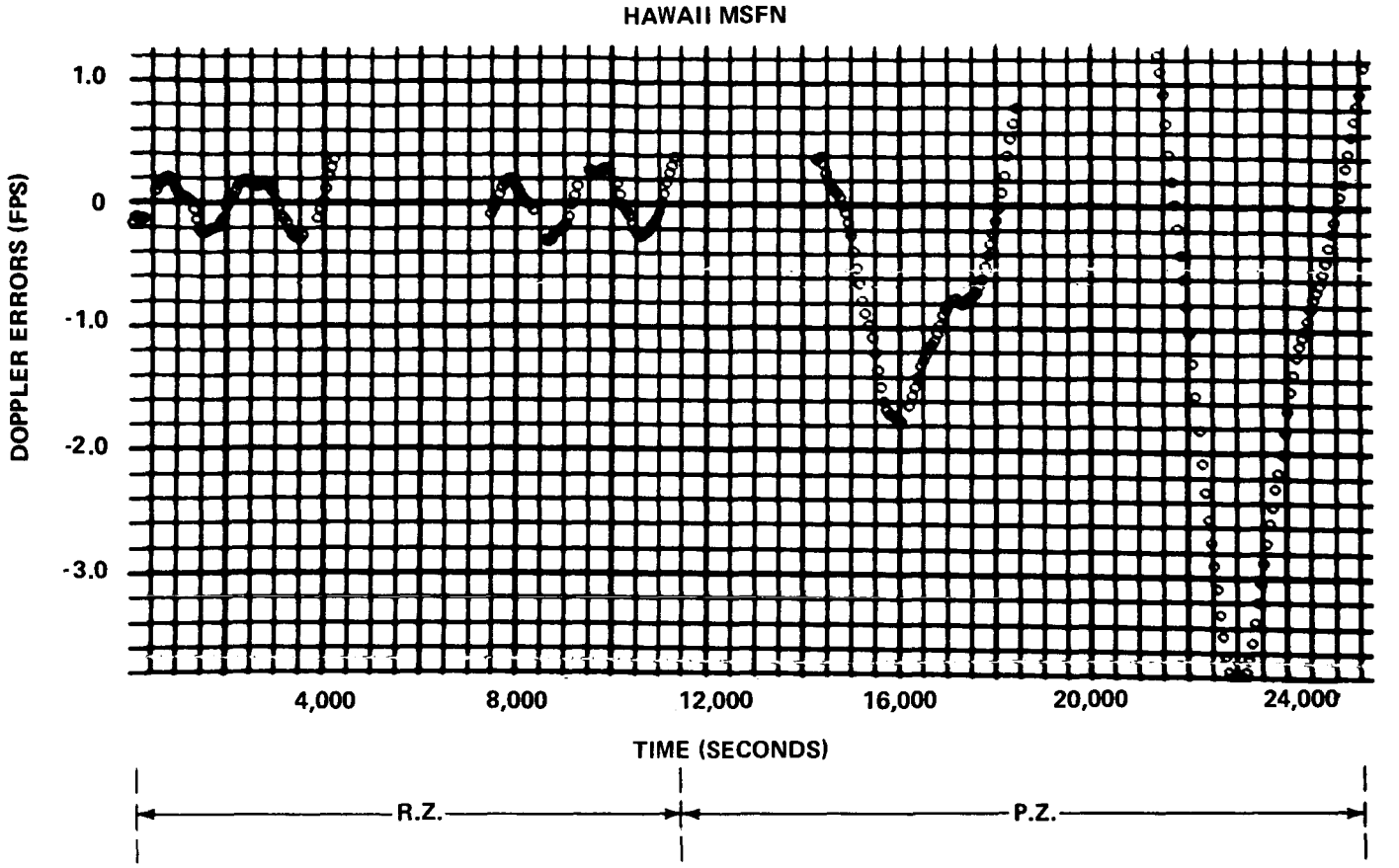

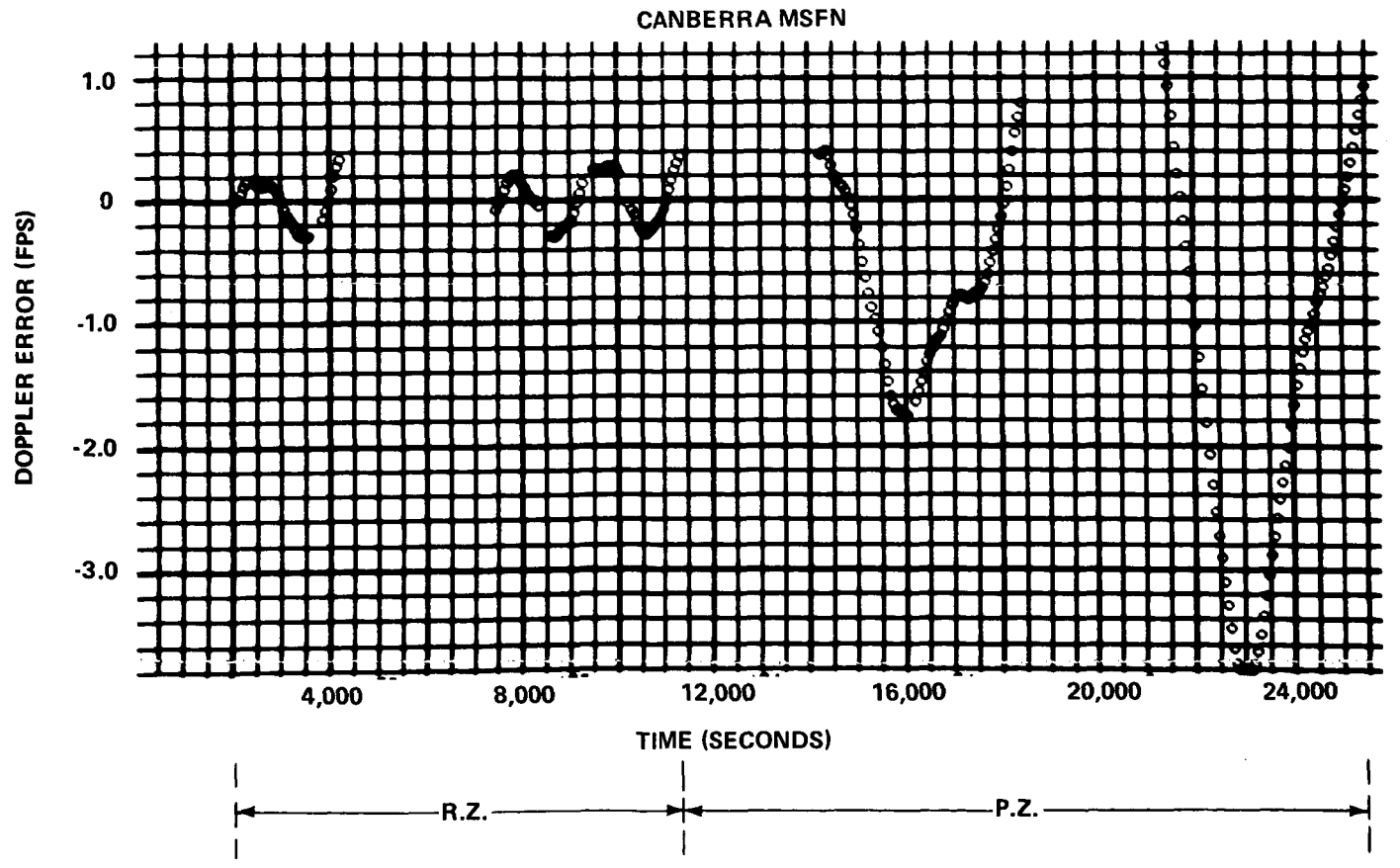

FIGURE 1- PASSES: 3,4 R.Z./5,6 P.Z.

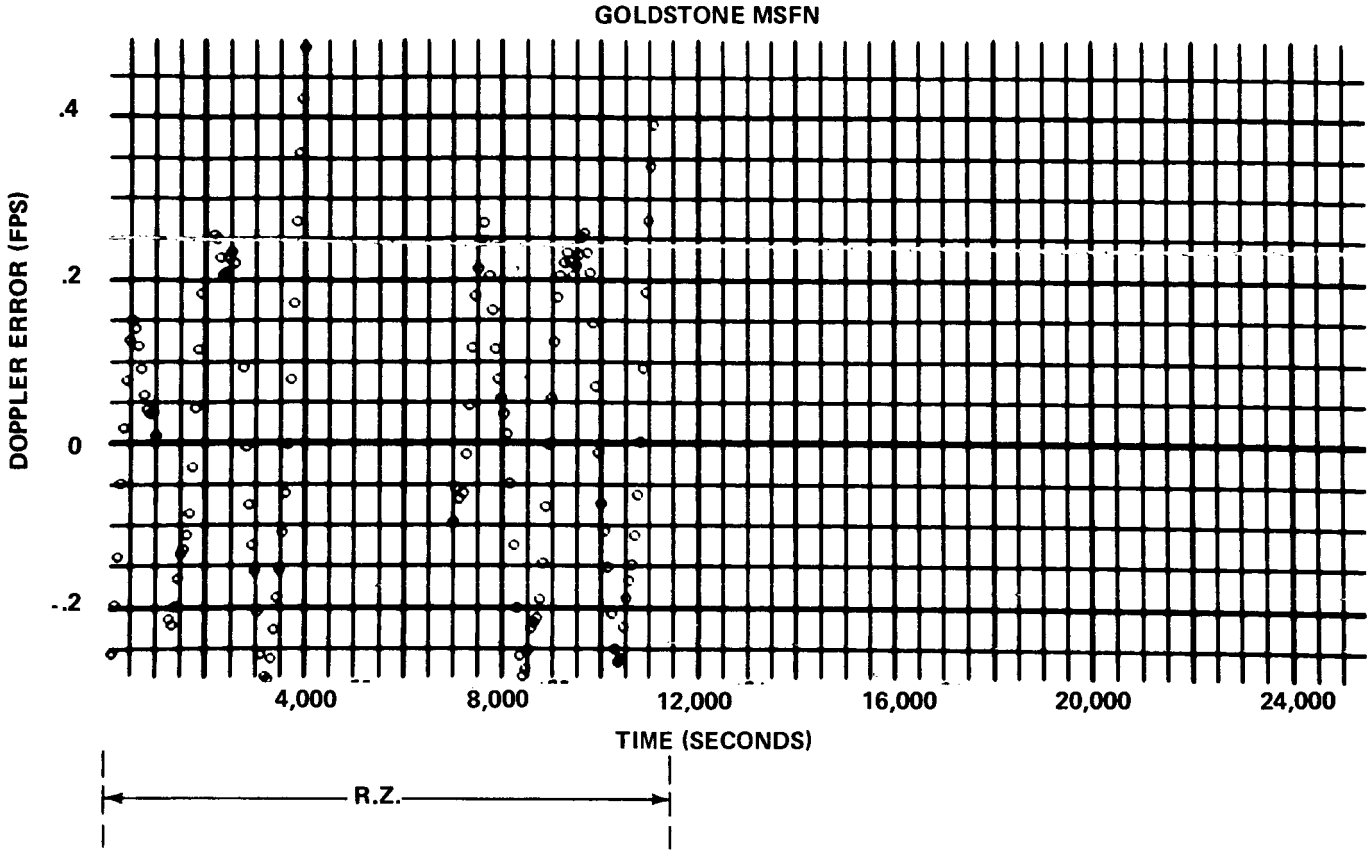

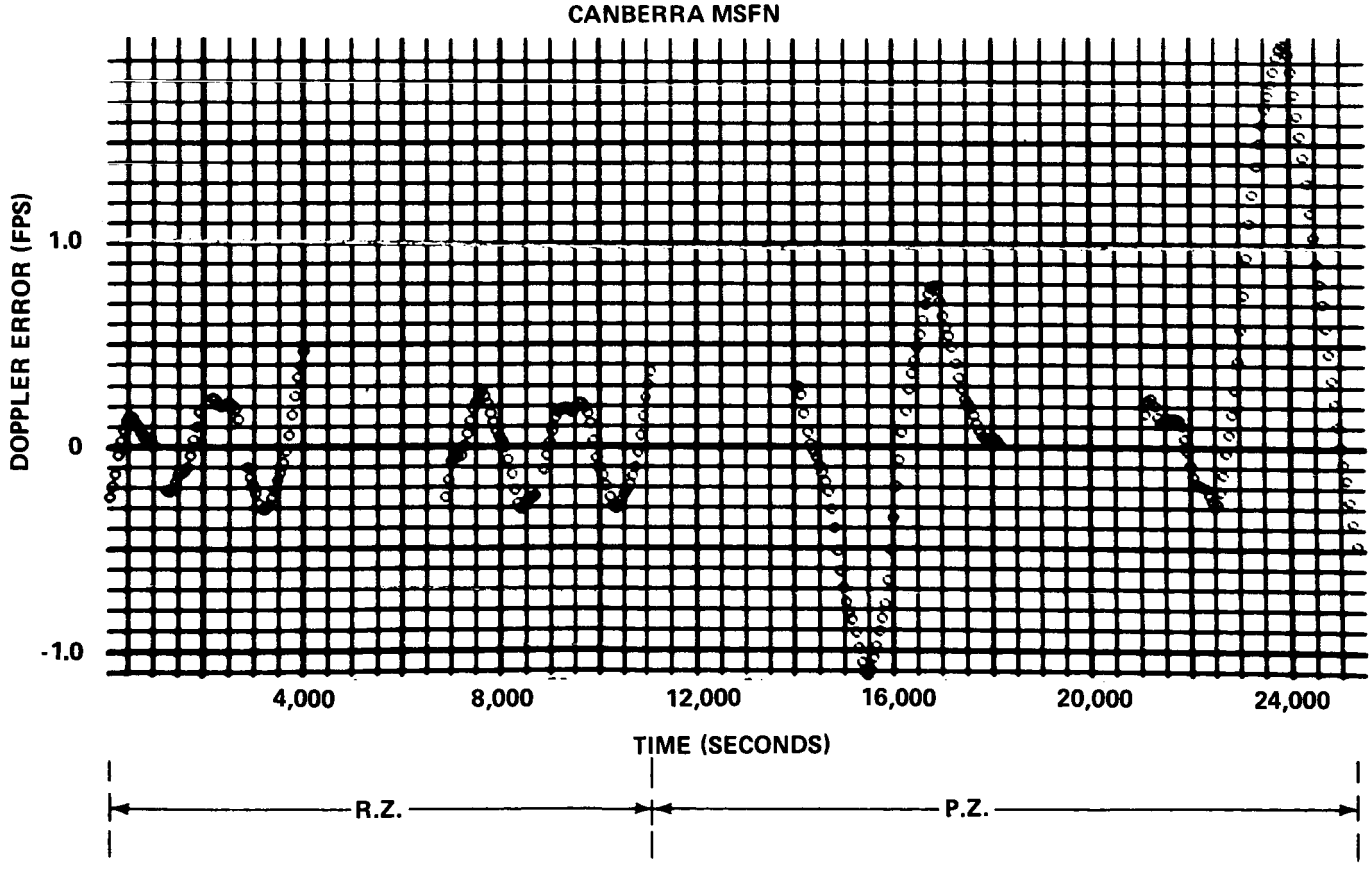

FIGURE 2- PASSES: 4,5 R.Z./6,7 P.Z.

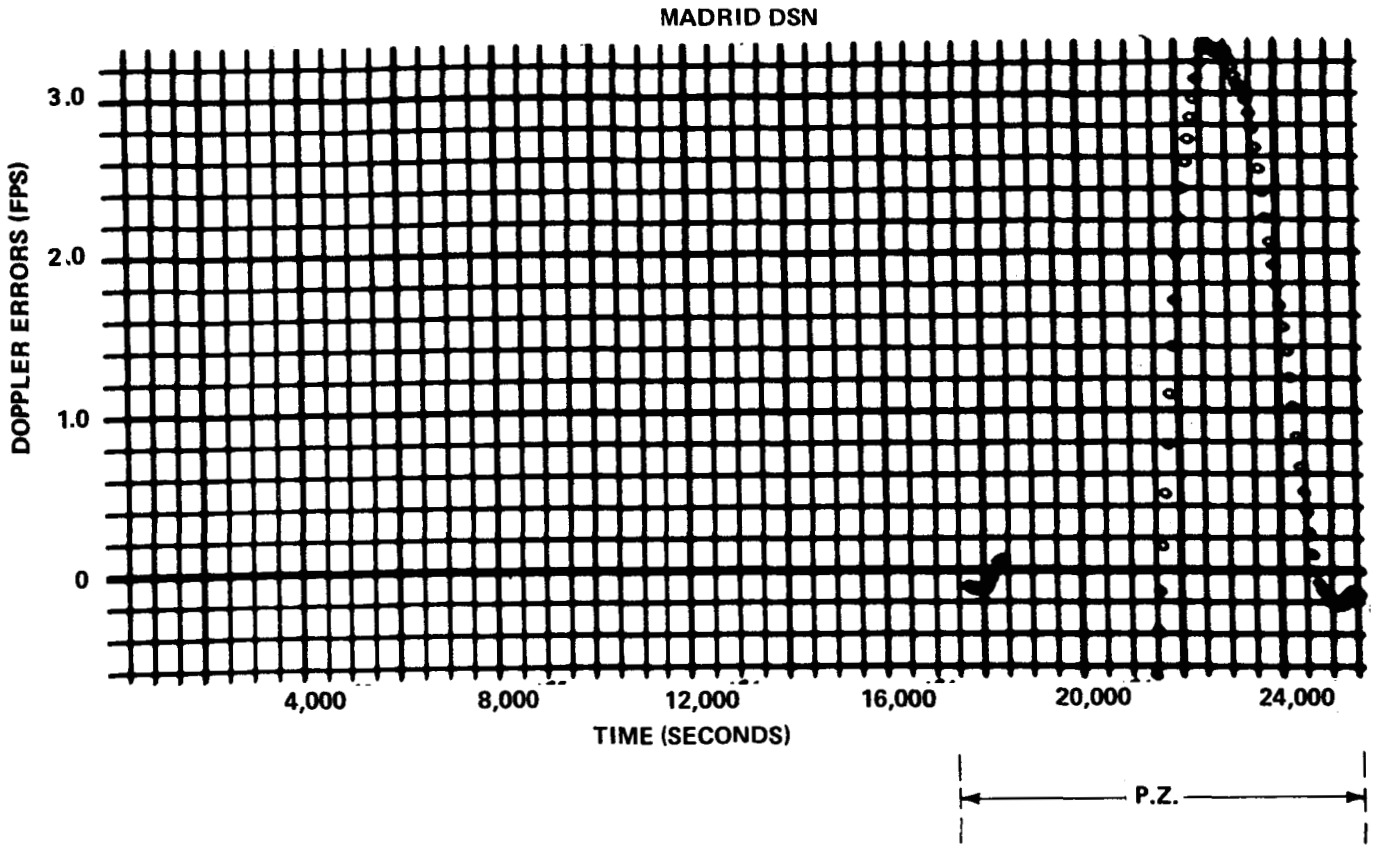

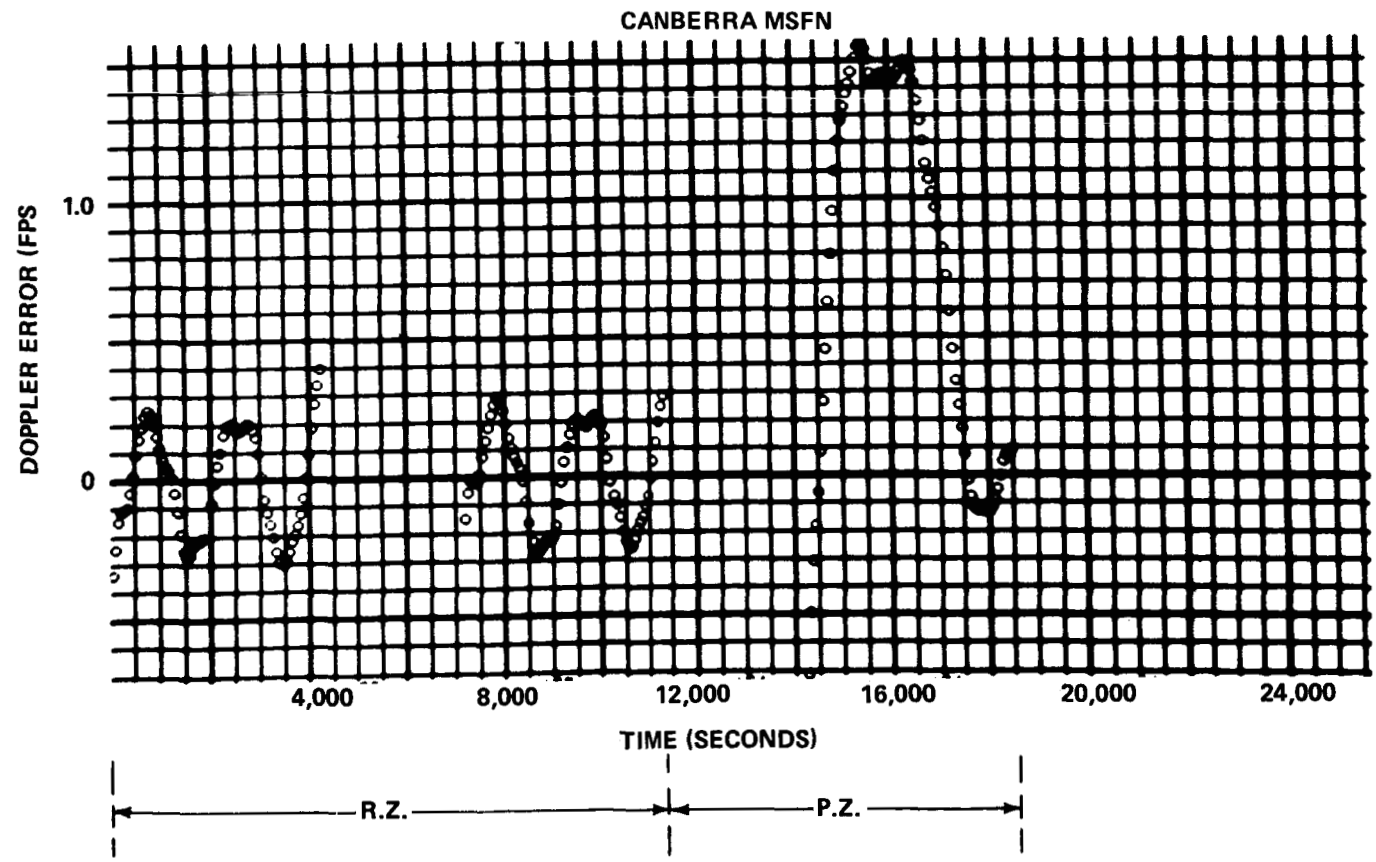

FIGURE 3- PASSES: 5,6 R.Z./7,8 P.Z.

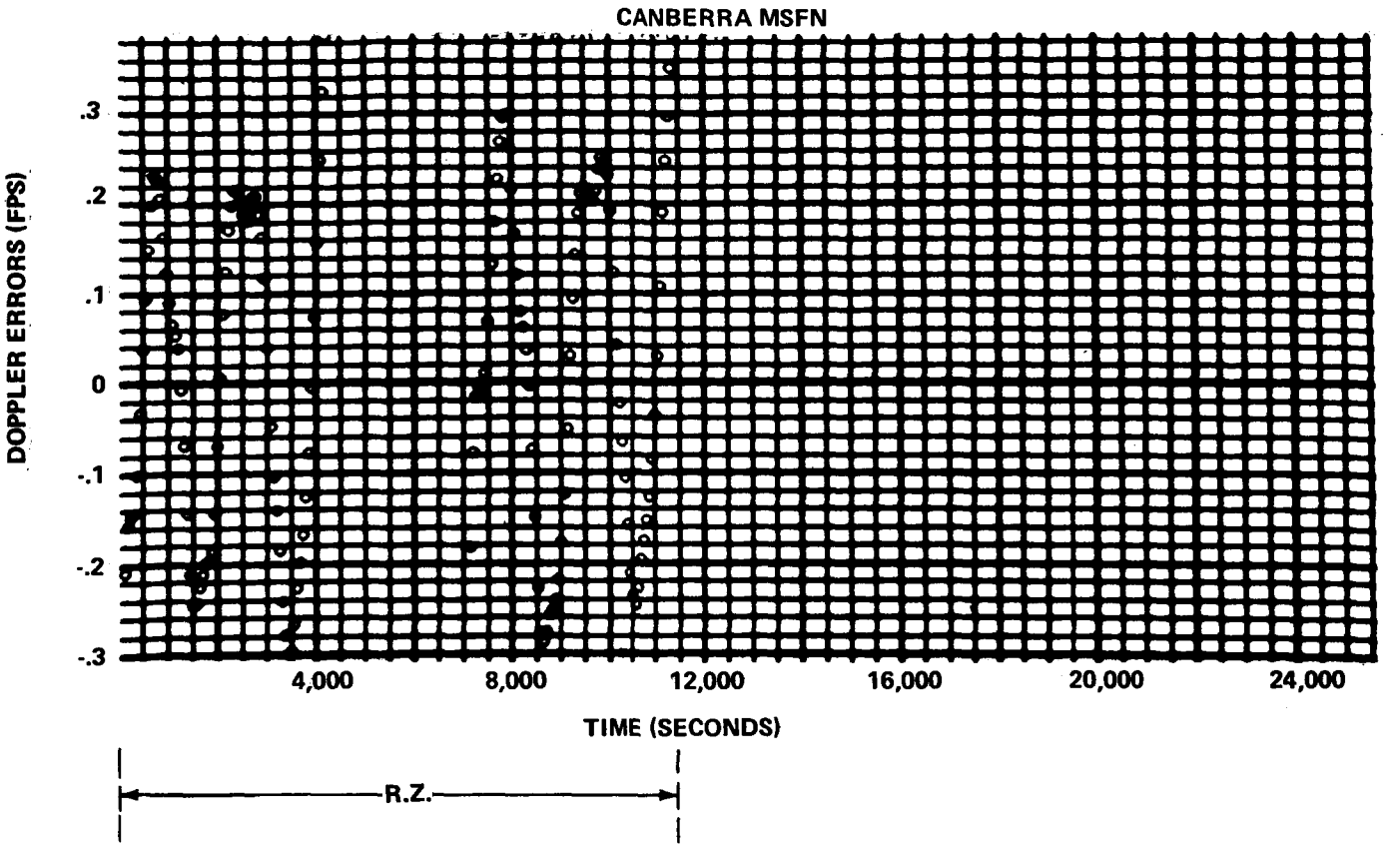

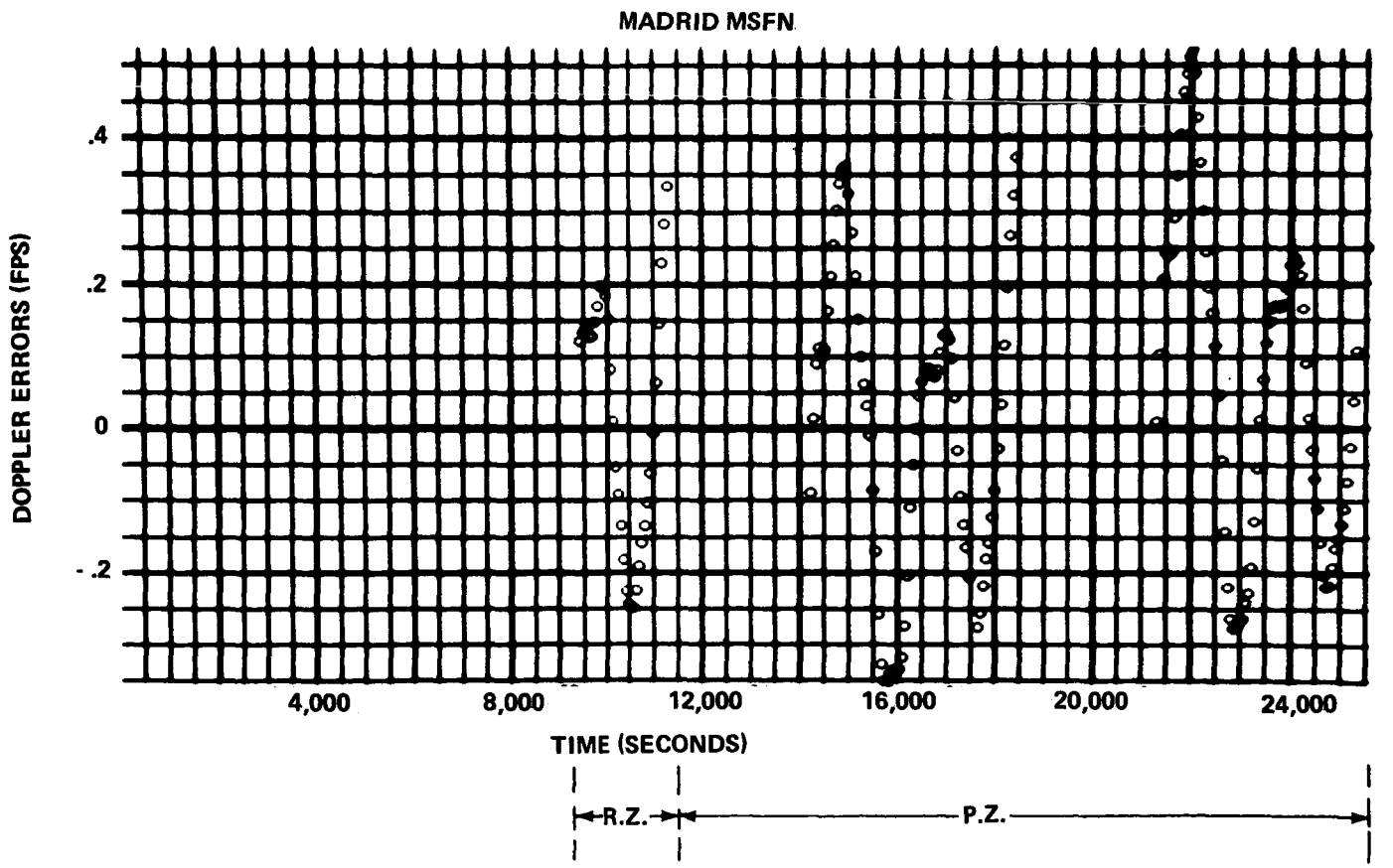

FIGURE 4- PASSES: 6,7 R.Z./8,9 P.Z.

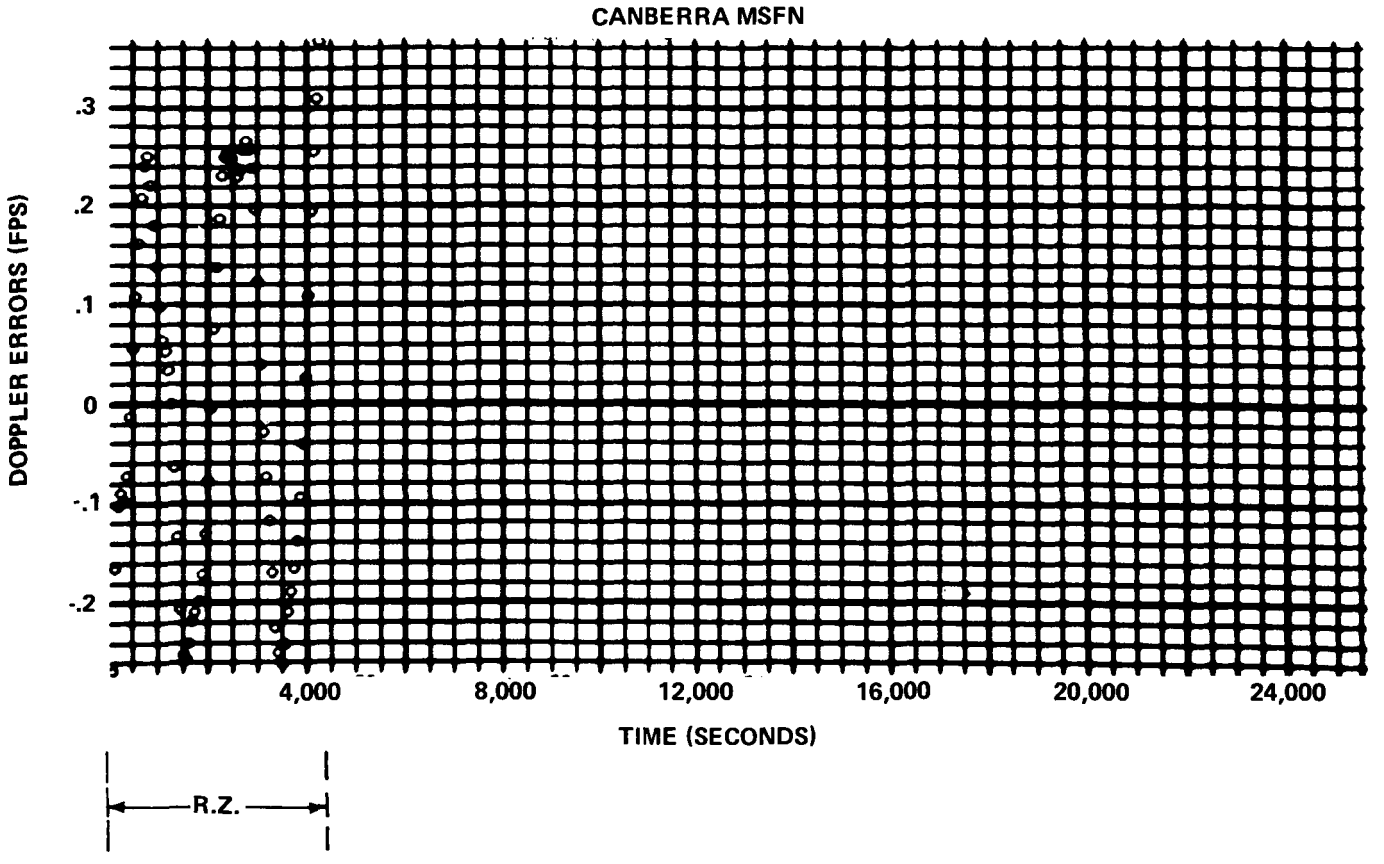

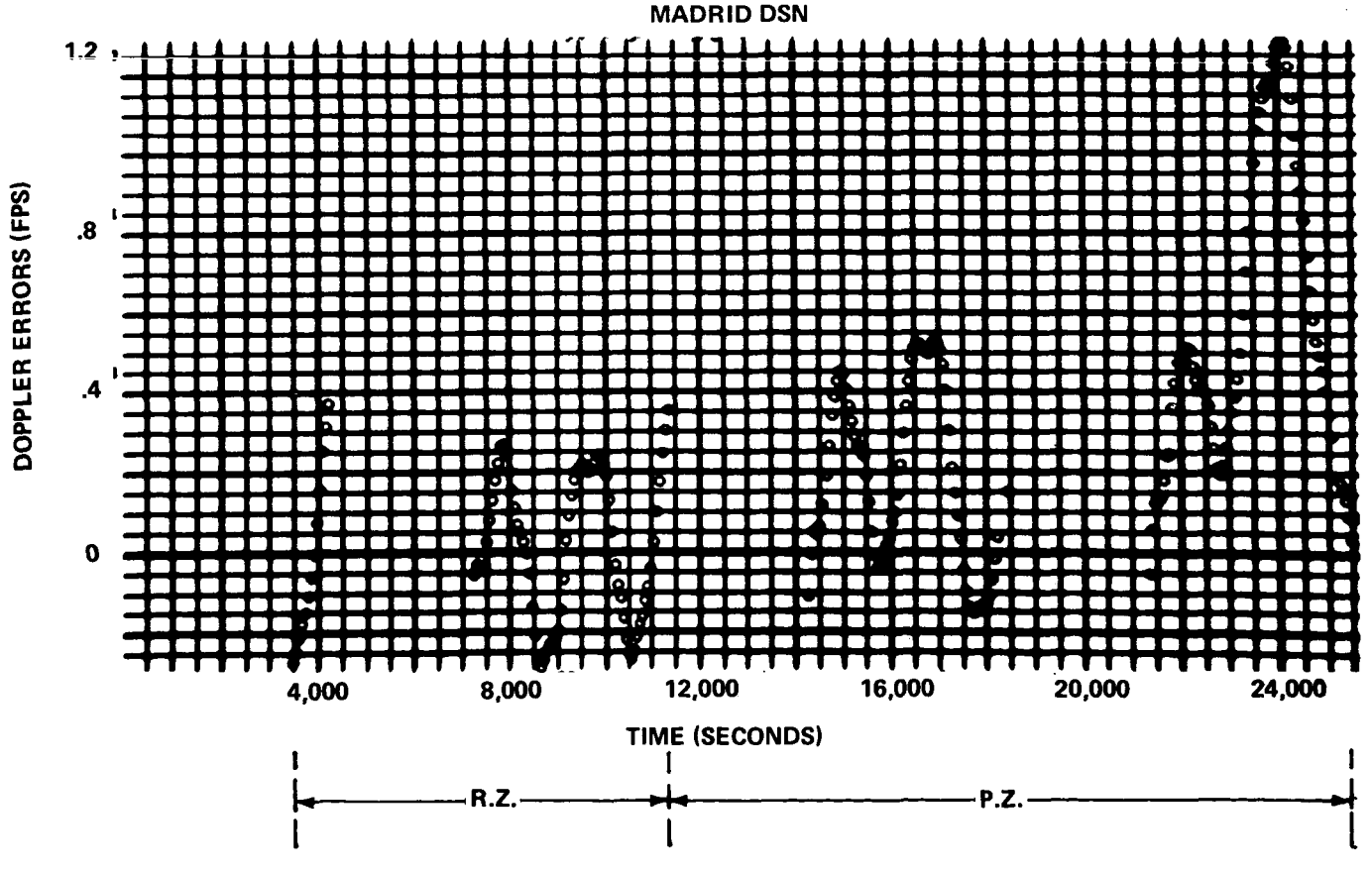

FIGURE 5- PASSES: 7,8R.Z./9,10 P.Z.

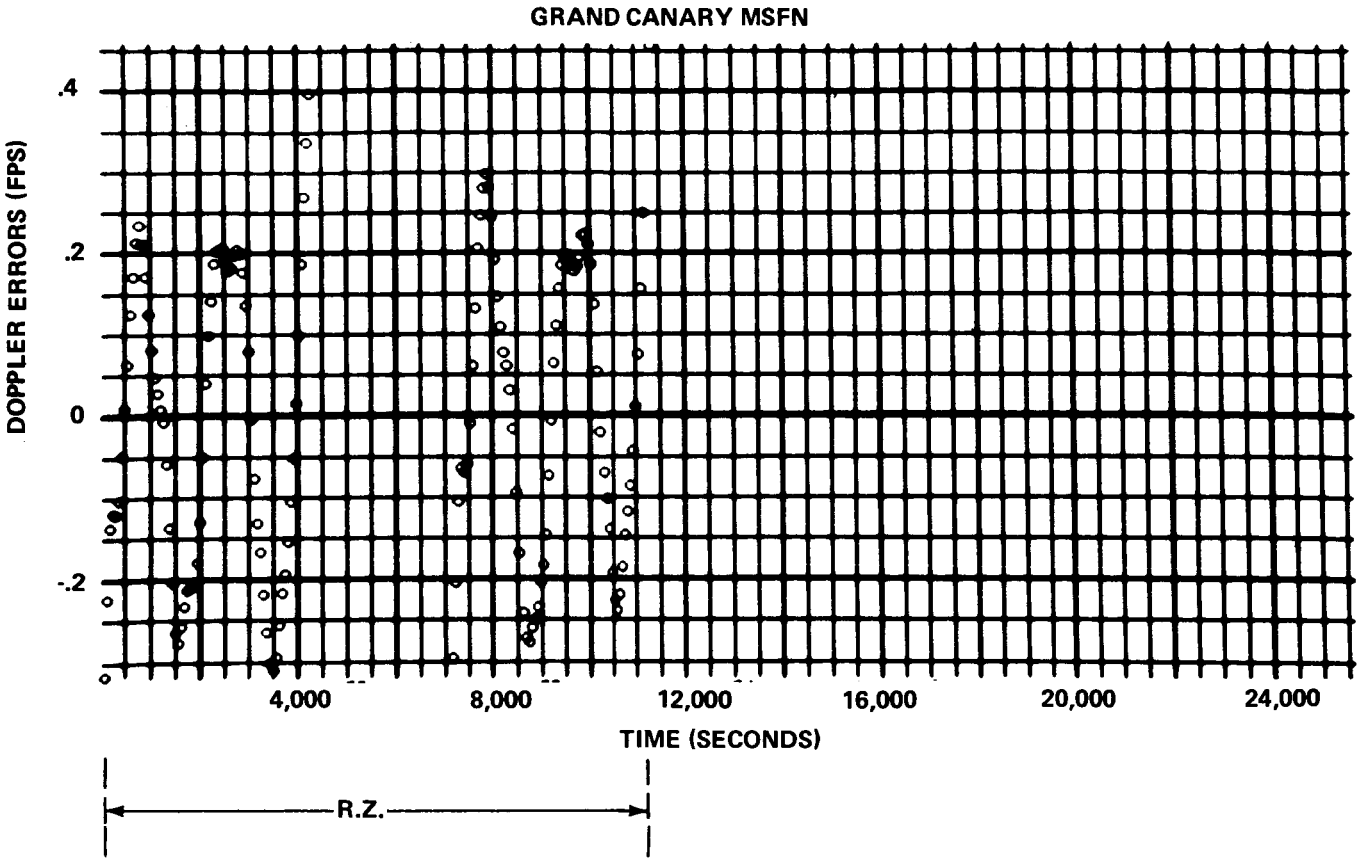

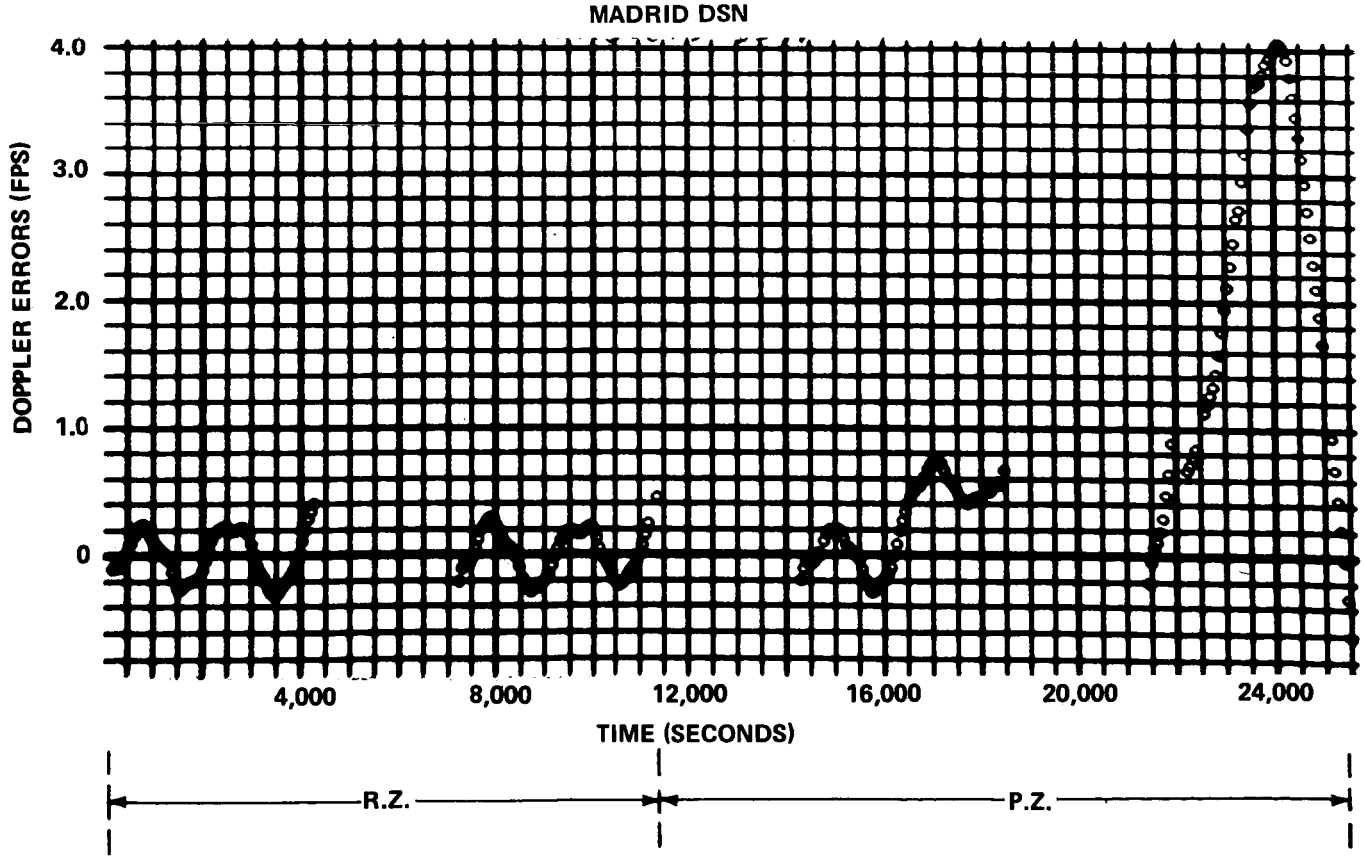

FIGURE 6- PASSES: 8,9 R.Z./10, 11 P.Z.

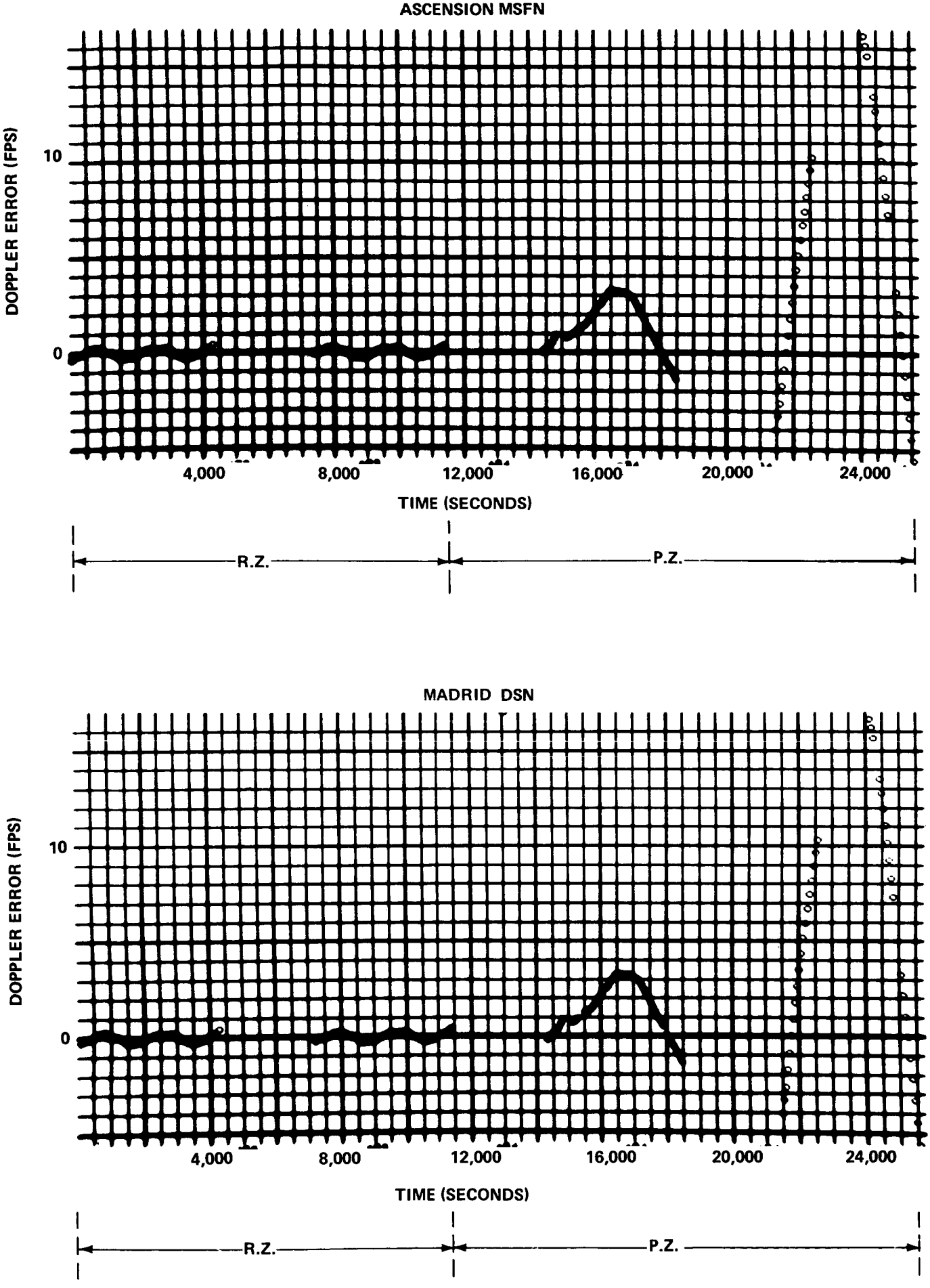

FIGURE 7- PASSES: 9,10 R.Z./11,12 P.Z.

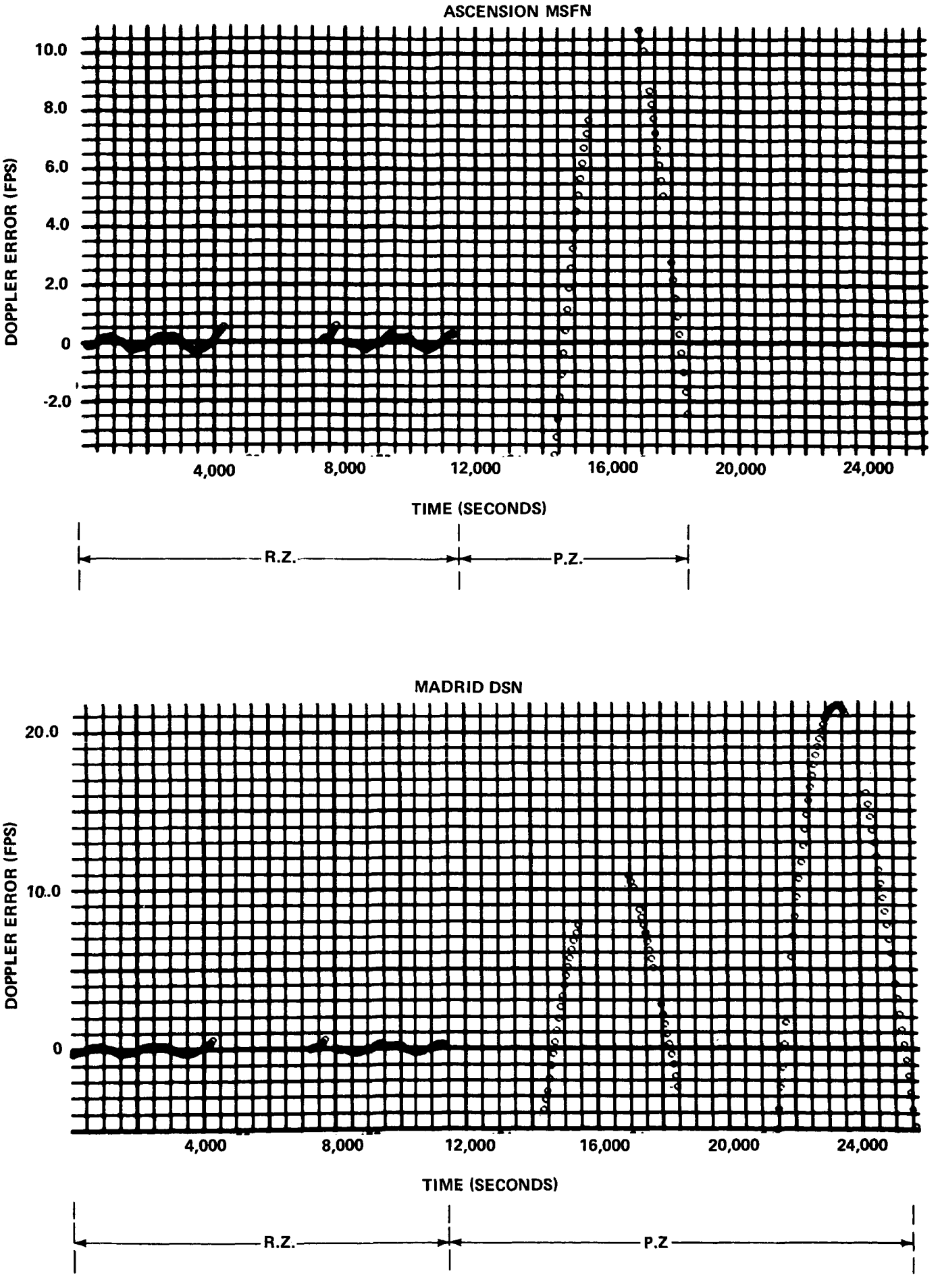

FIGURE 8 - PASSES: 10,11 R.Z./ 12,13 P.Z.

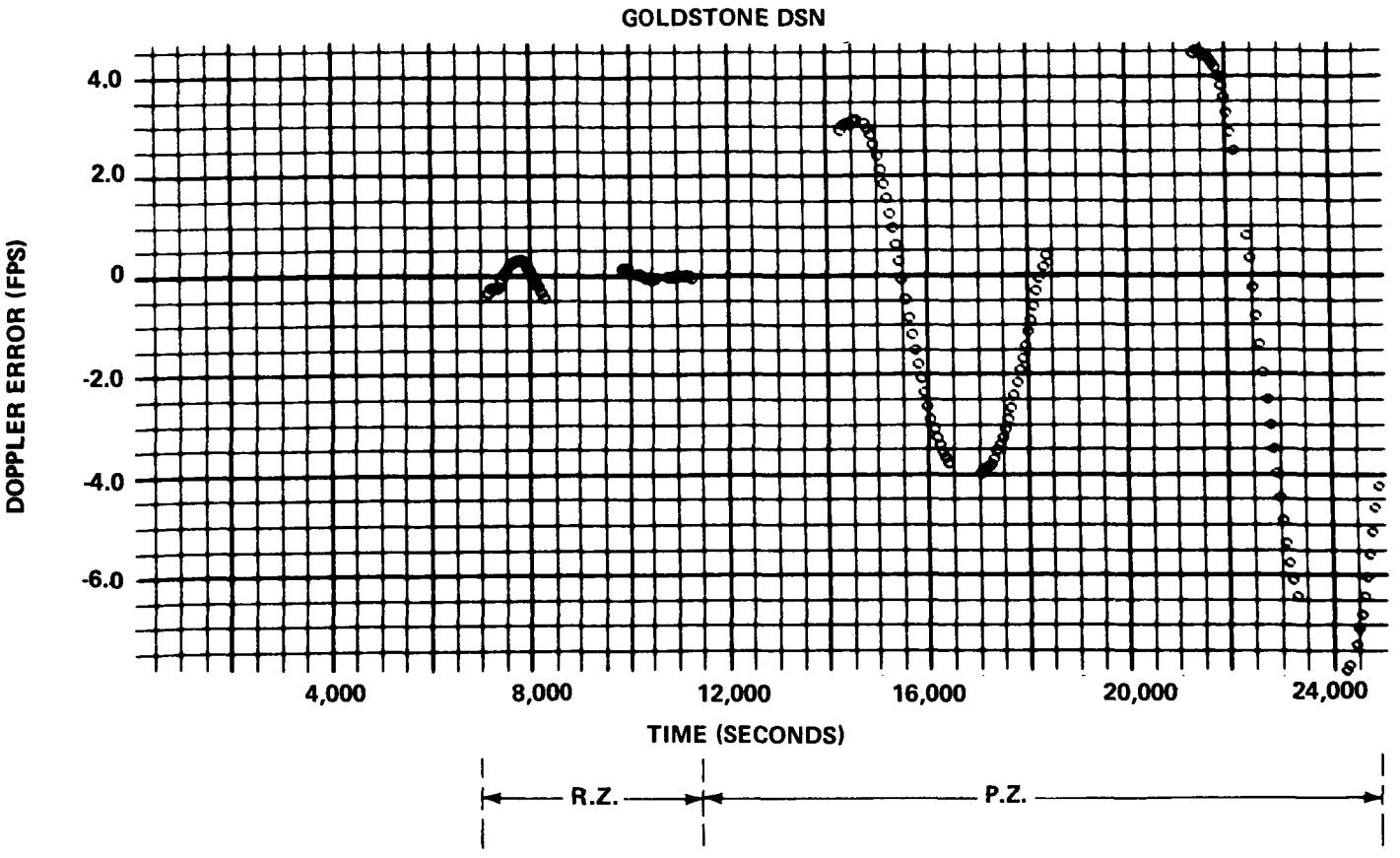

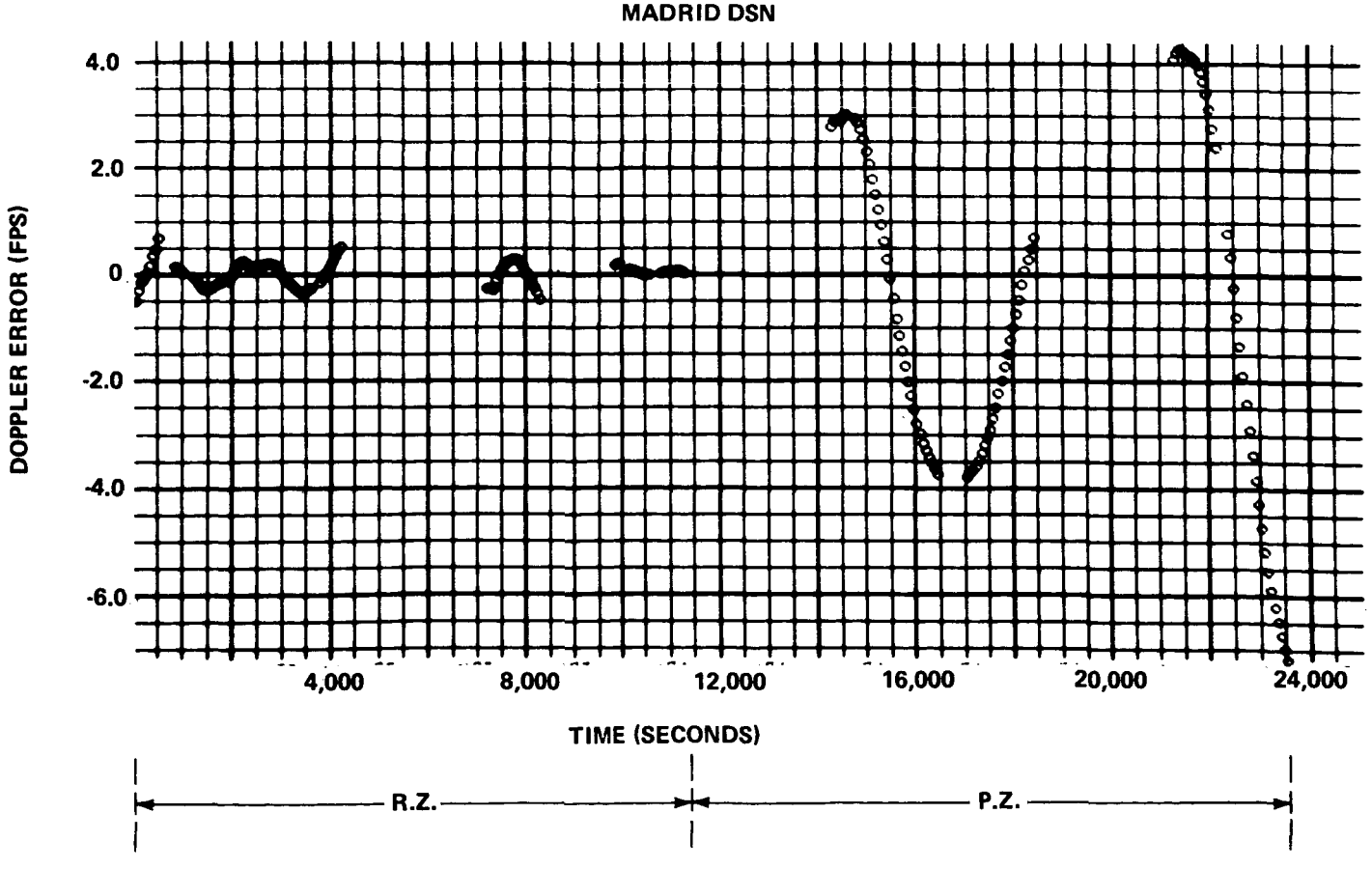

FIGURE 9 - PASSES: 11,12 R.Z./13,14 P.Z.

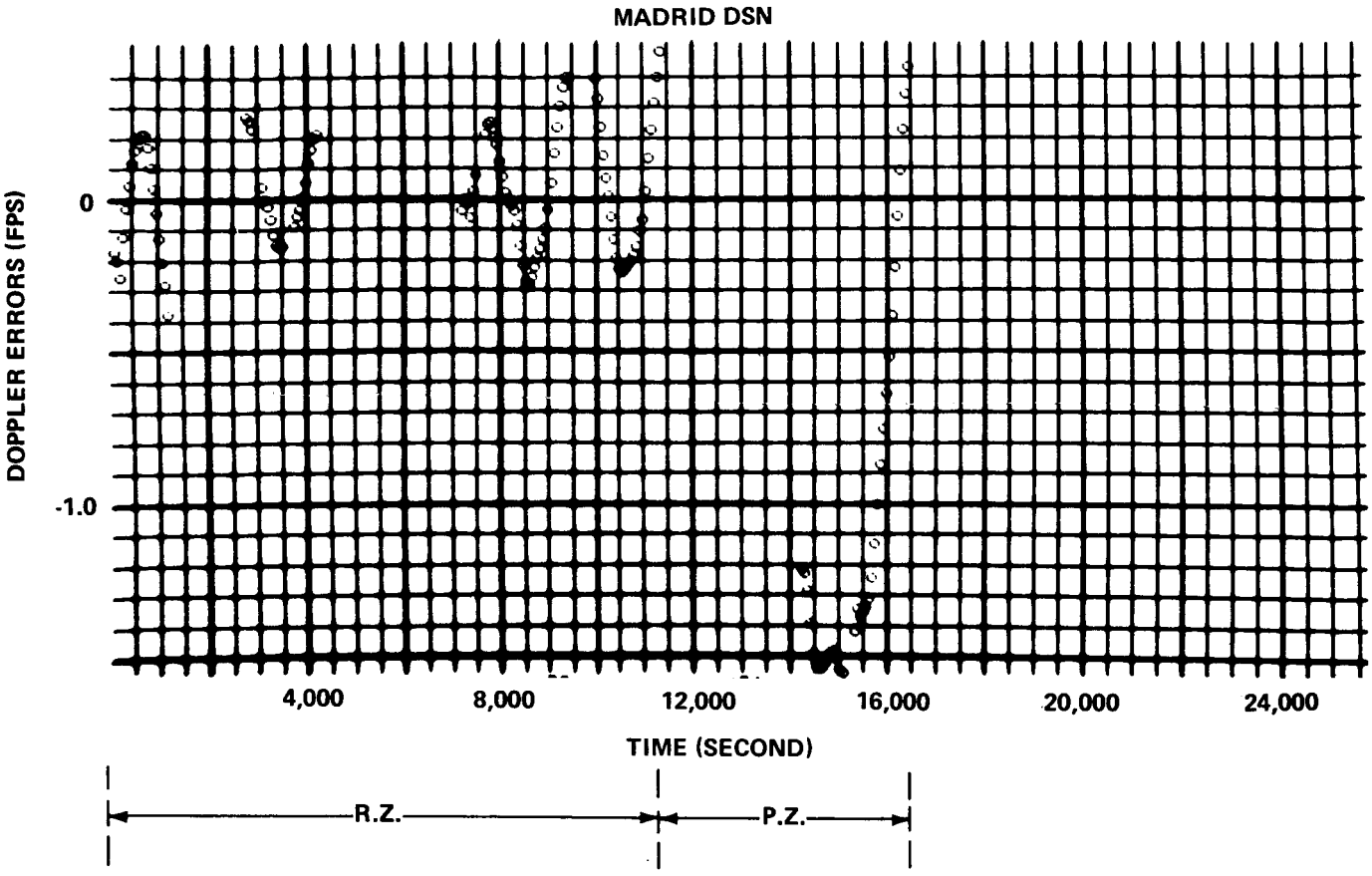

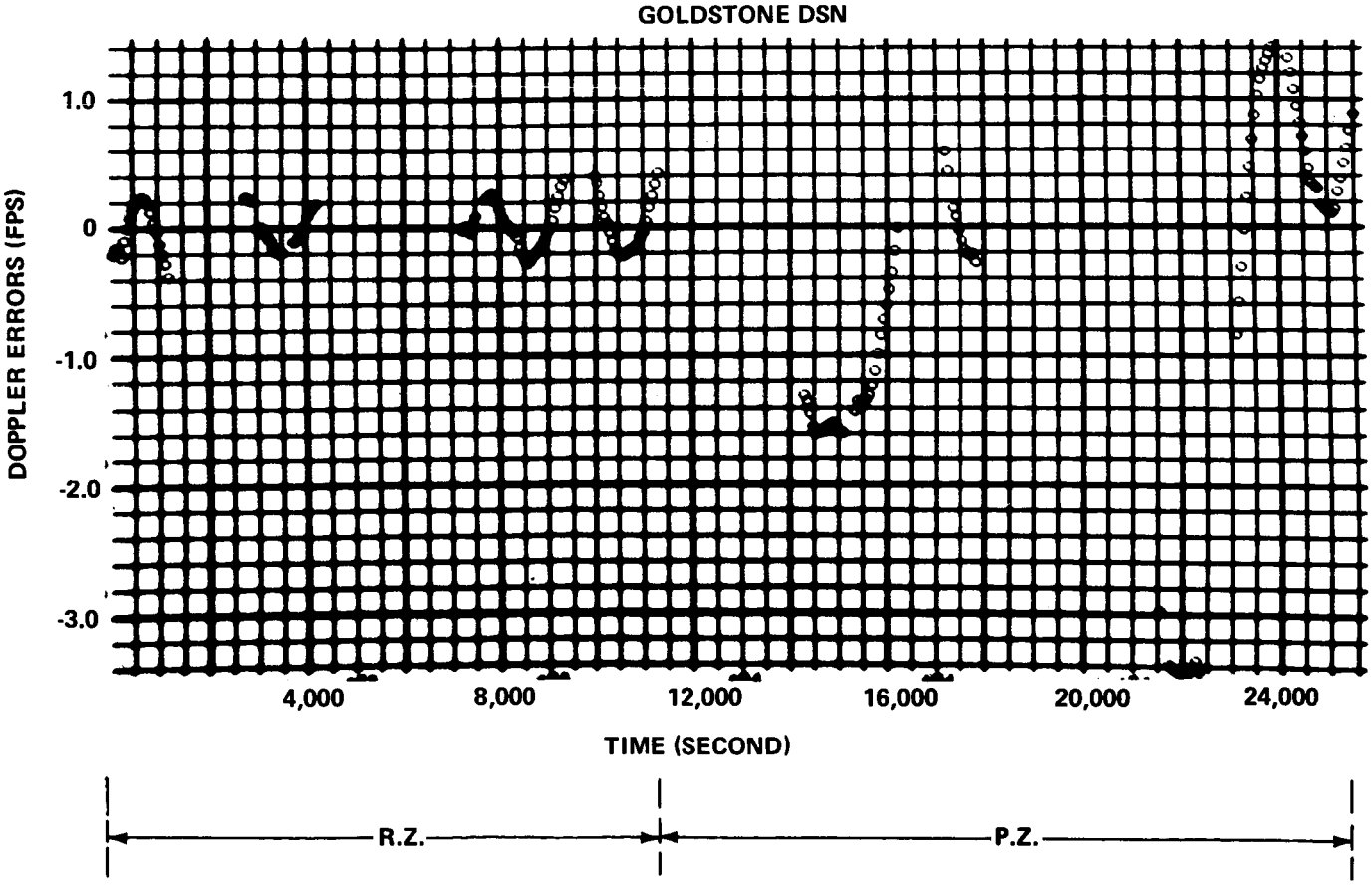

FIGURE 10- PASSES: 12,13 R.Z./14,15 P.Z.

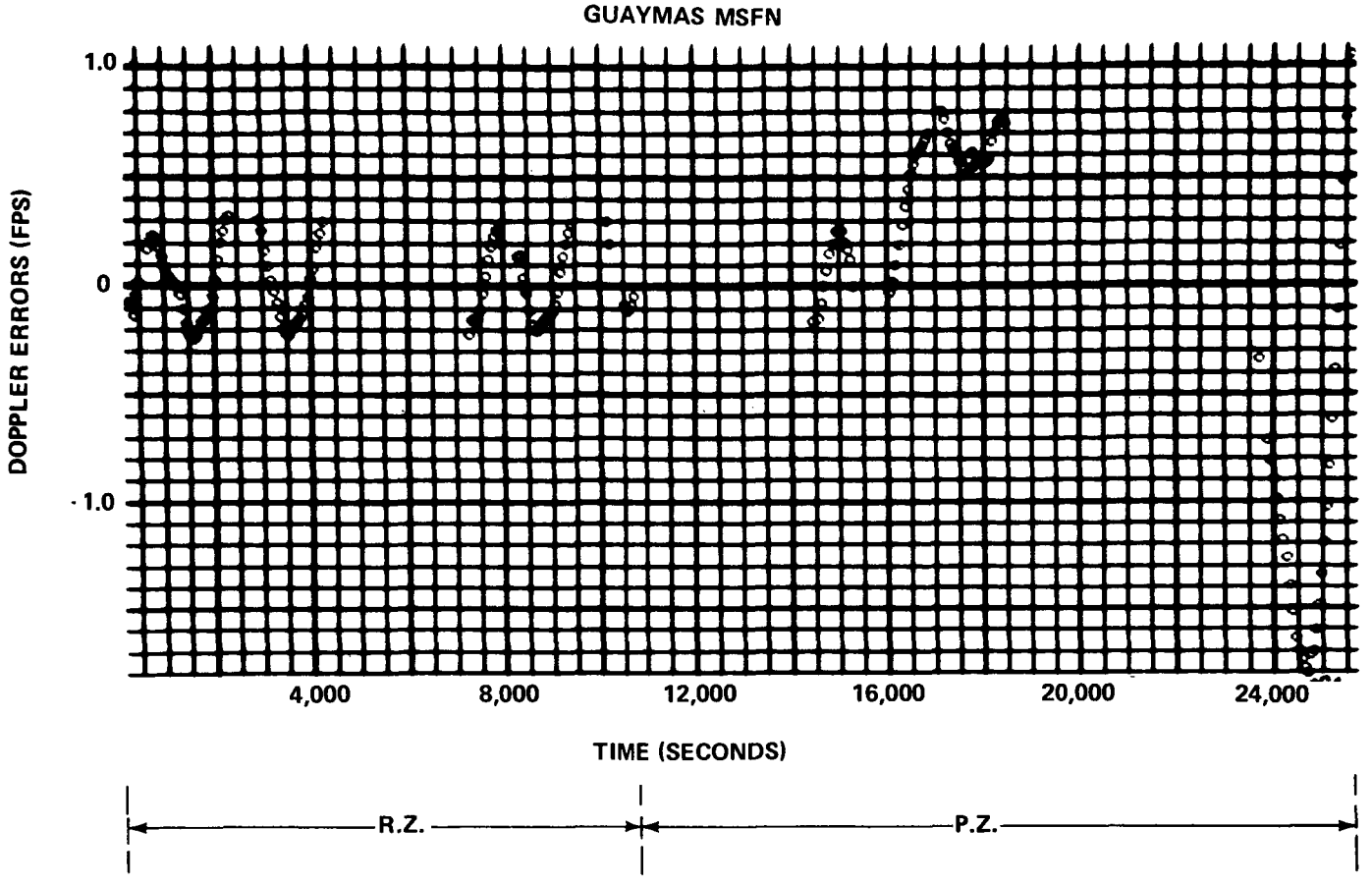

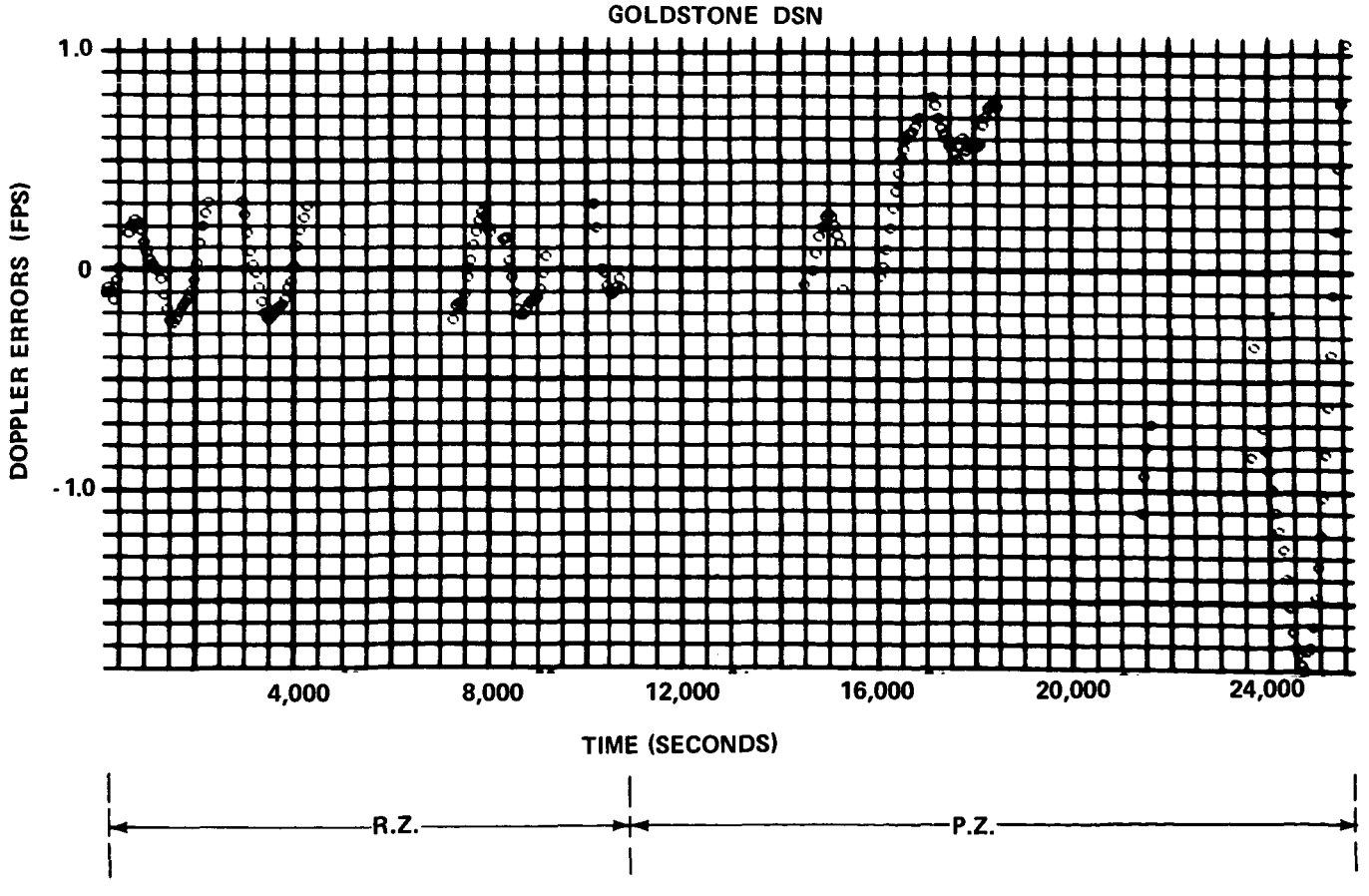

FIGURE 11- PASSES: 13,14 R.Z./ 15,16 P.Z.

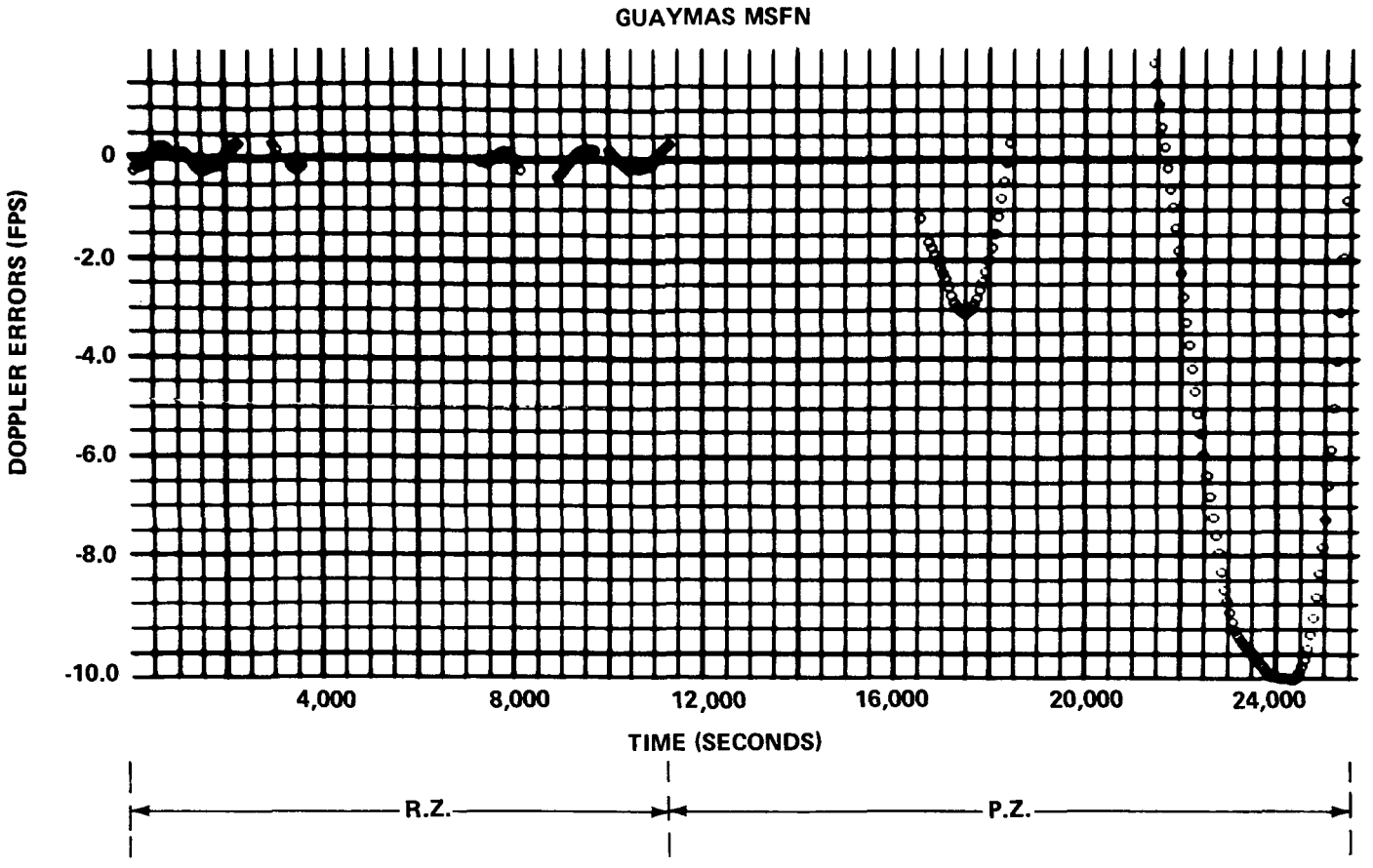

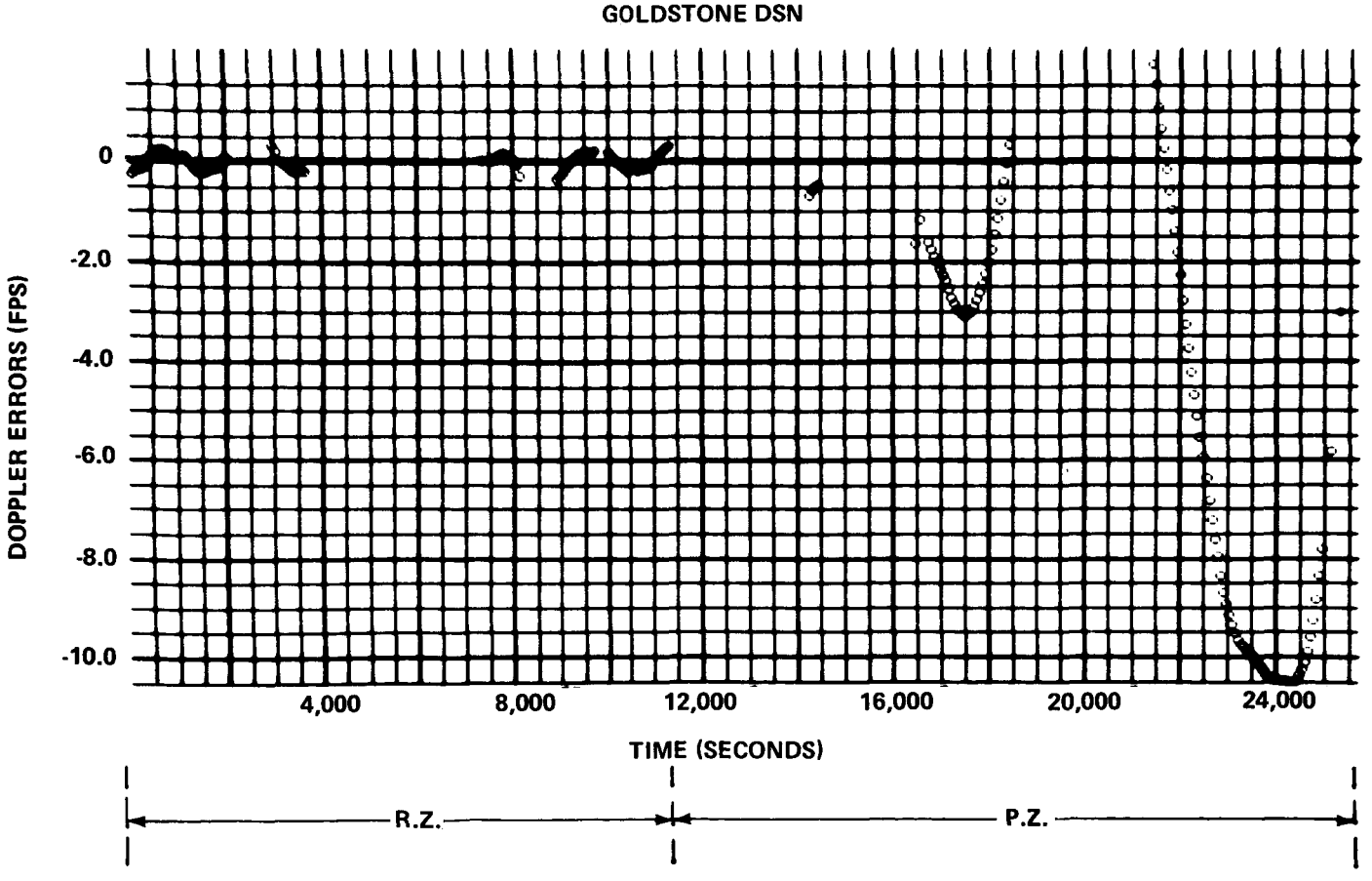

FIGURE 12- PASSES: 14,15 R.Z./16,17 P.Z.

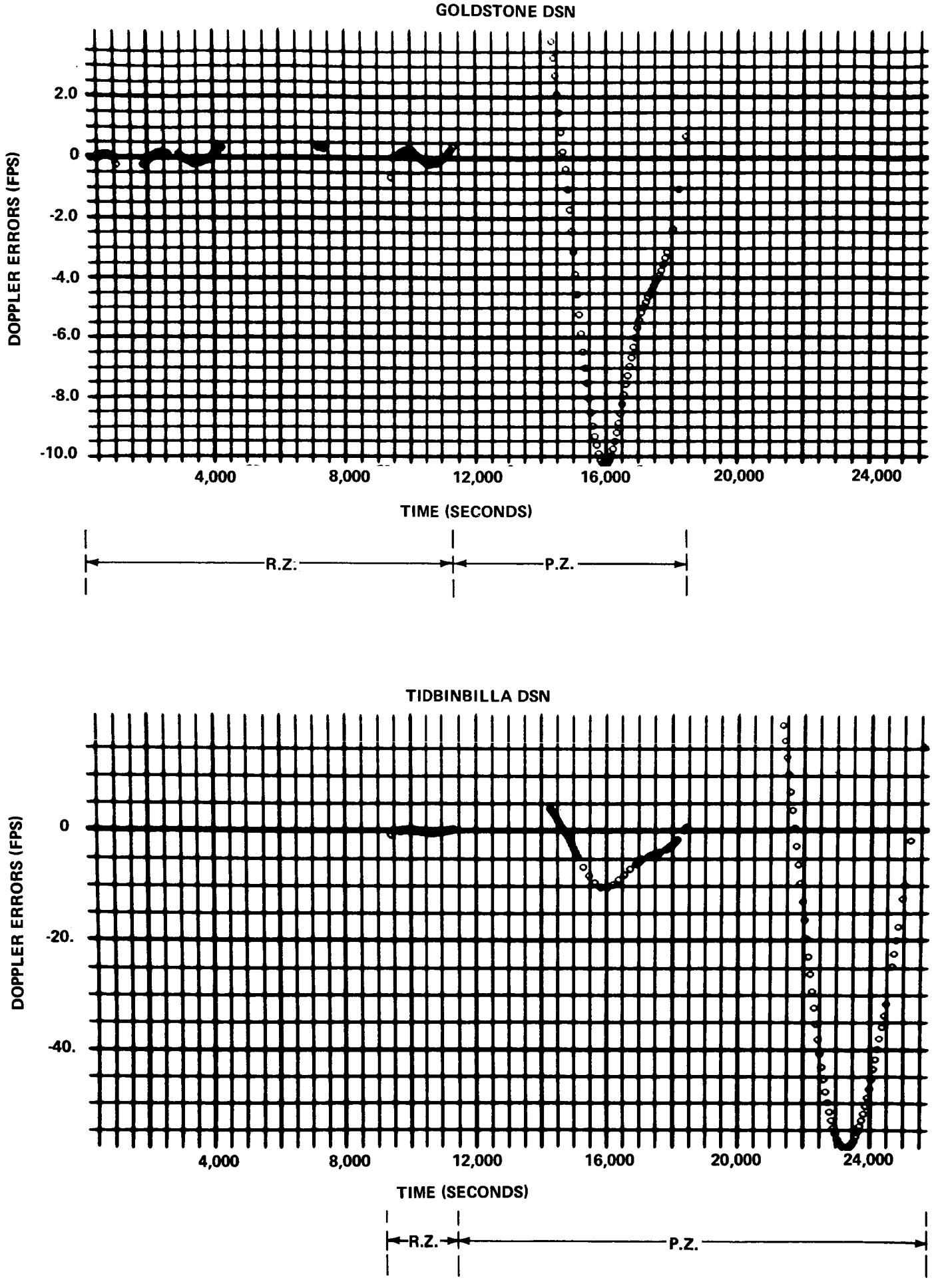

FIGURE 13- PASSES: 15,16 R.Z./17,18 P.Z.

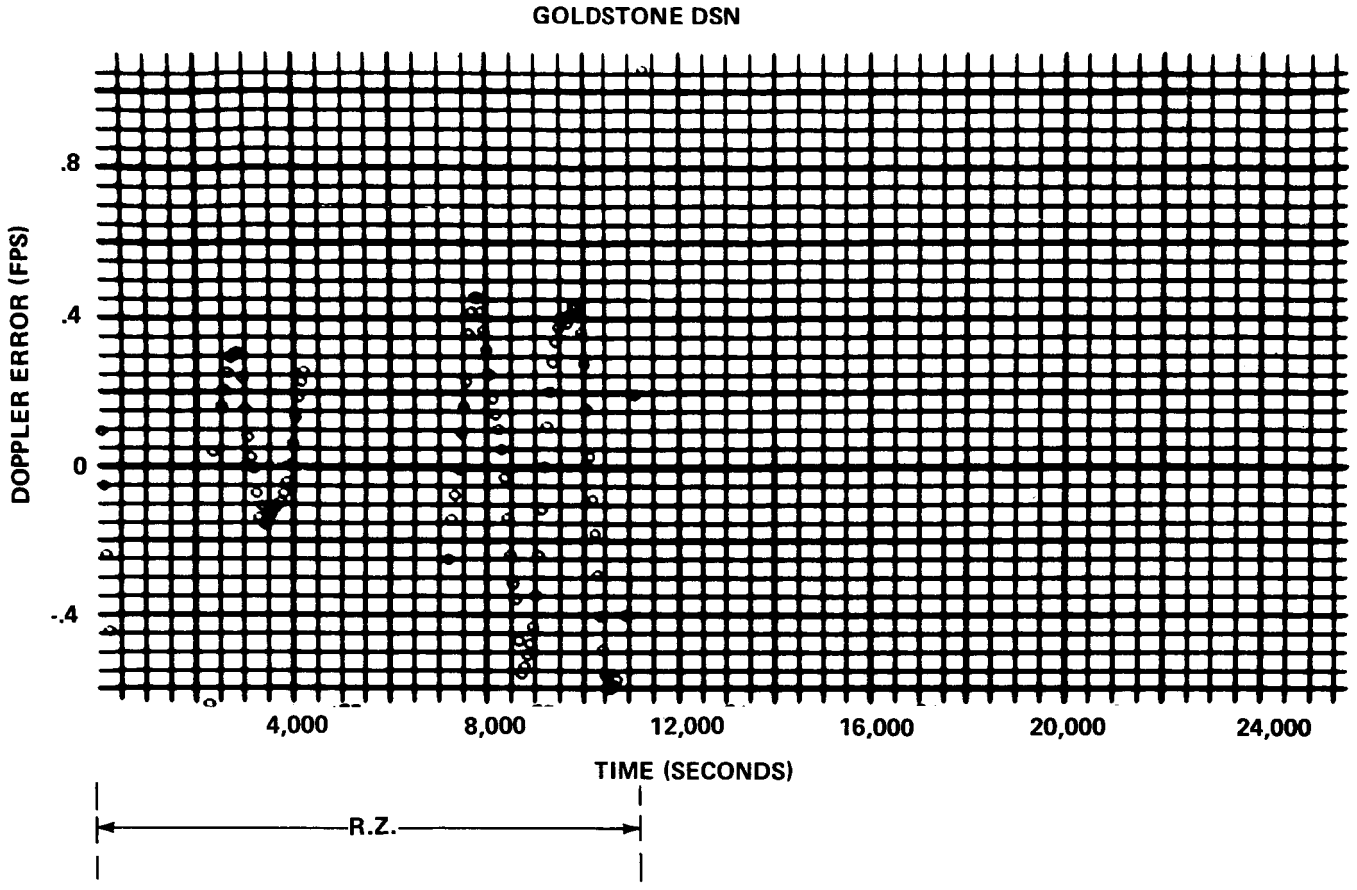

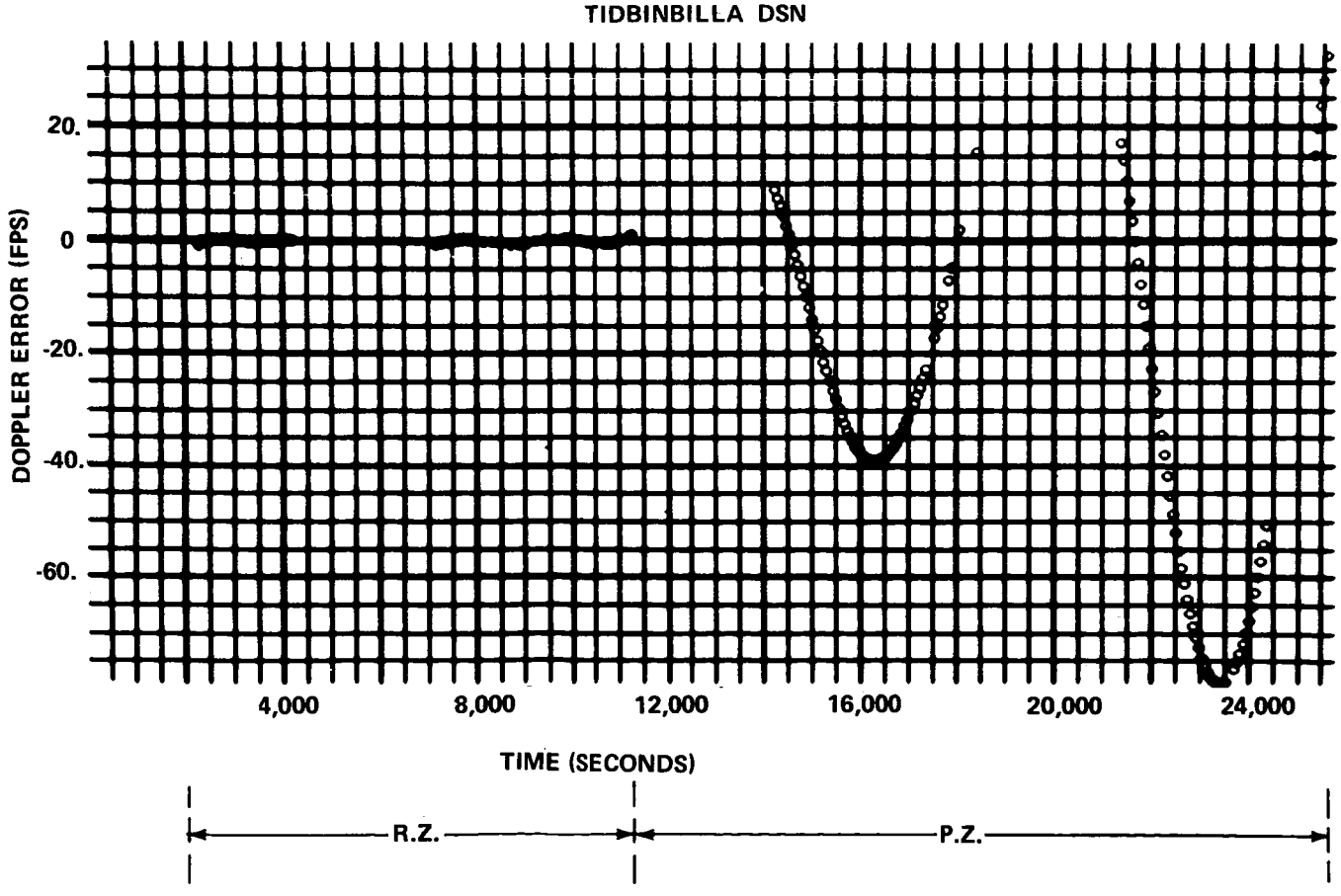

FIGURE 14- PASSES: 16,17 R.Z./18,19 P.Z.

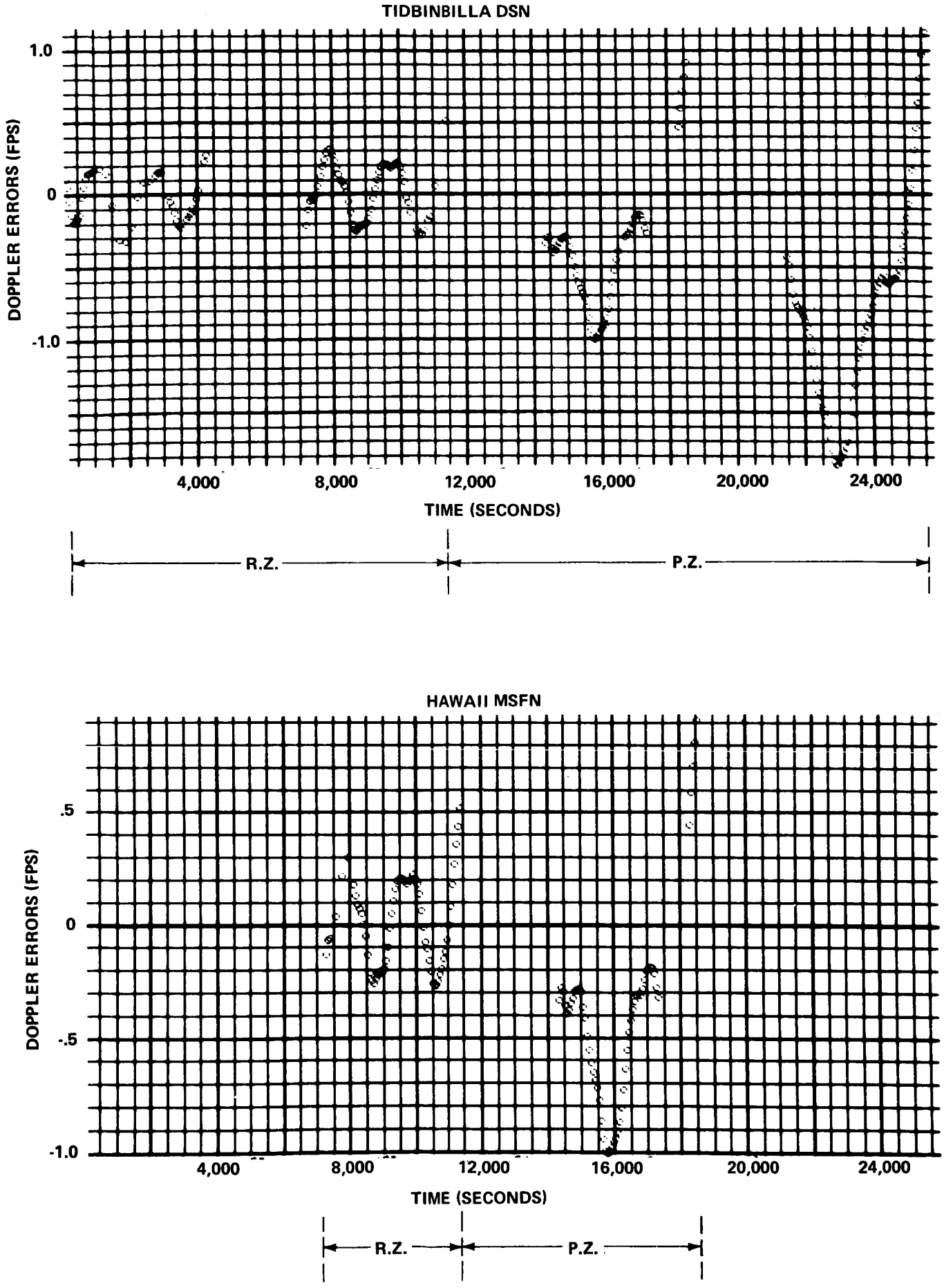

FIGURE 15- PASSES: 17,18 R.Z./19,20 P.Z.

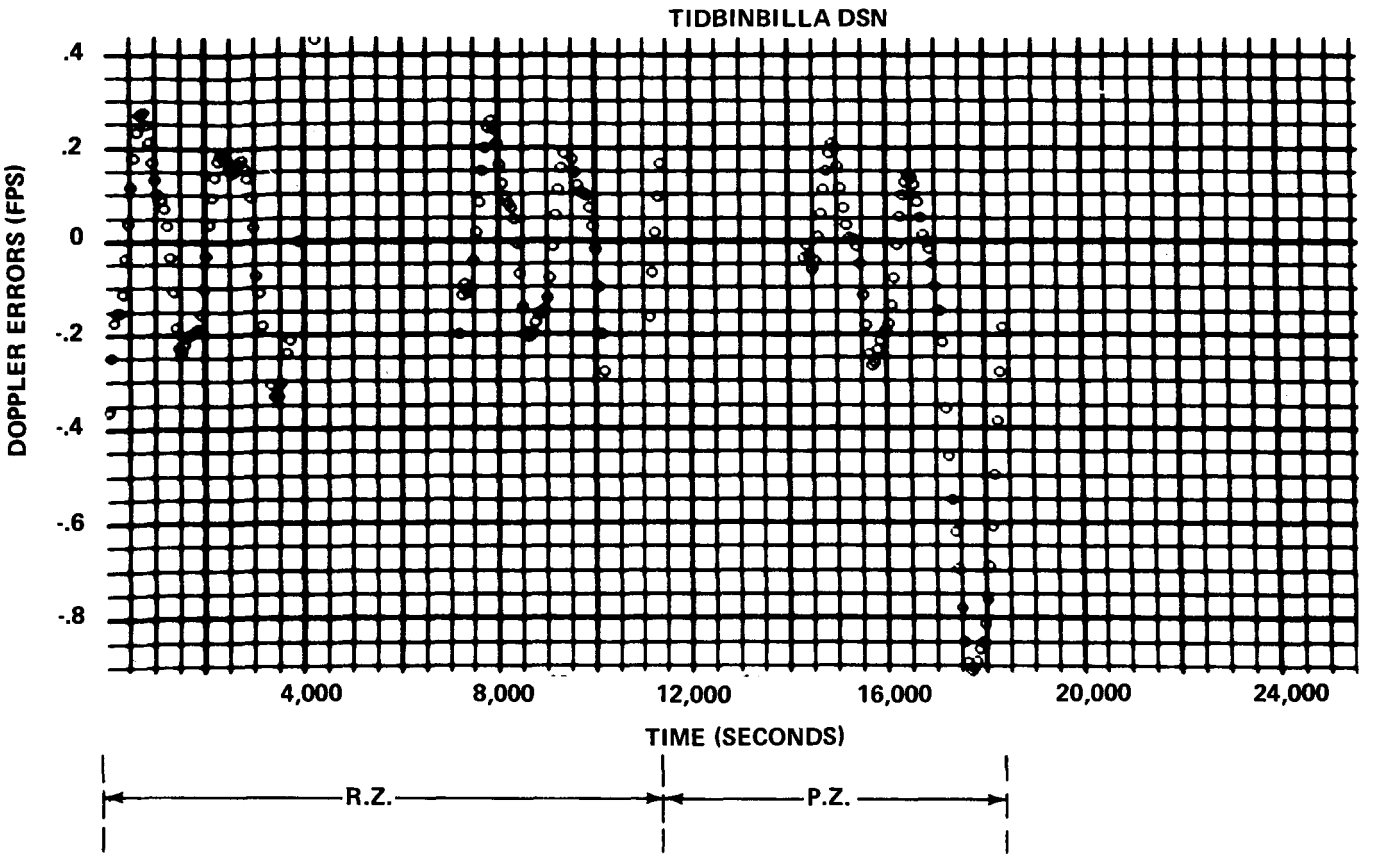

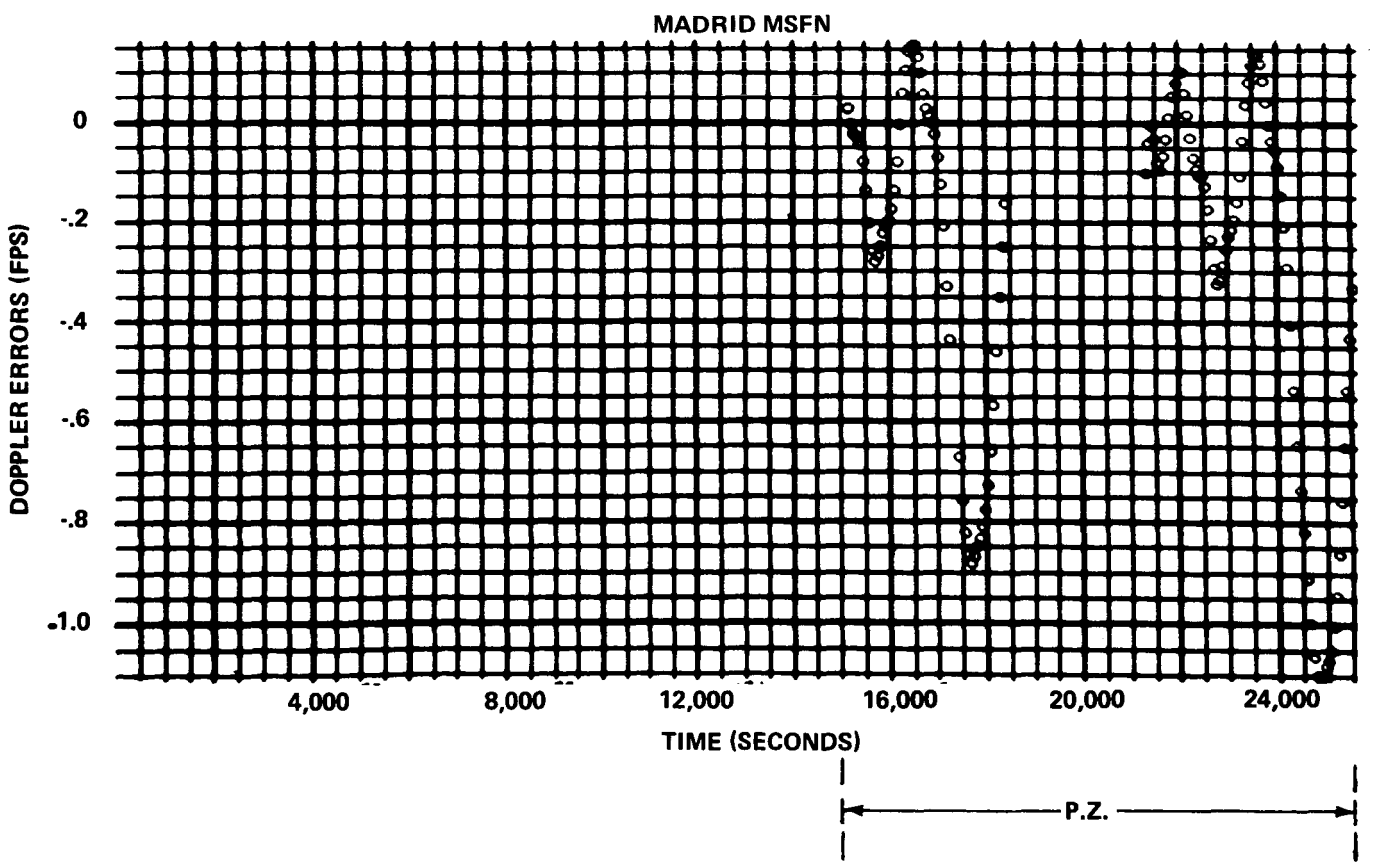

FIGURE 16- PASSES: 18,19 R.Z./20,21 P.Z.

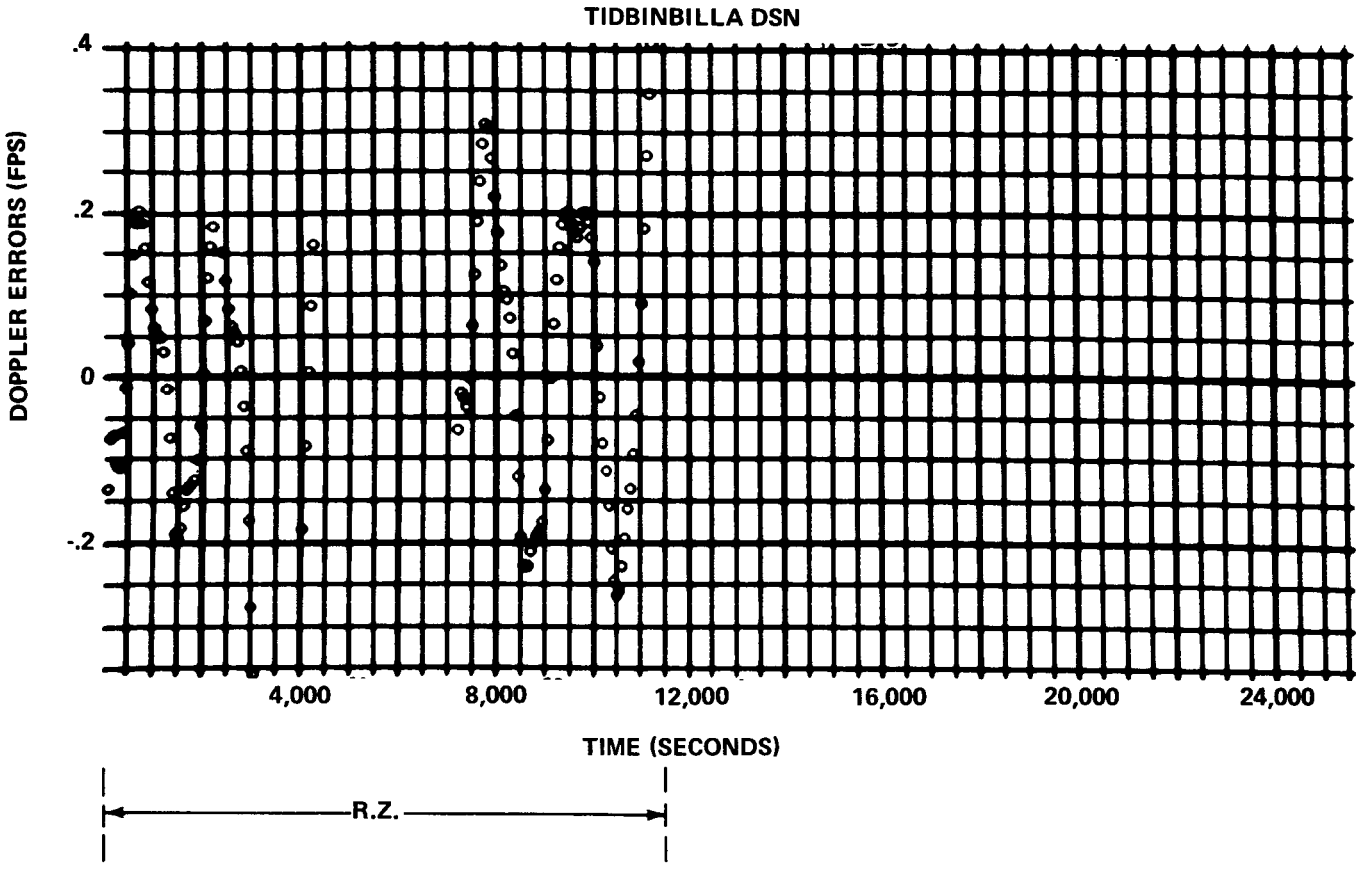

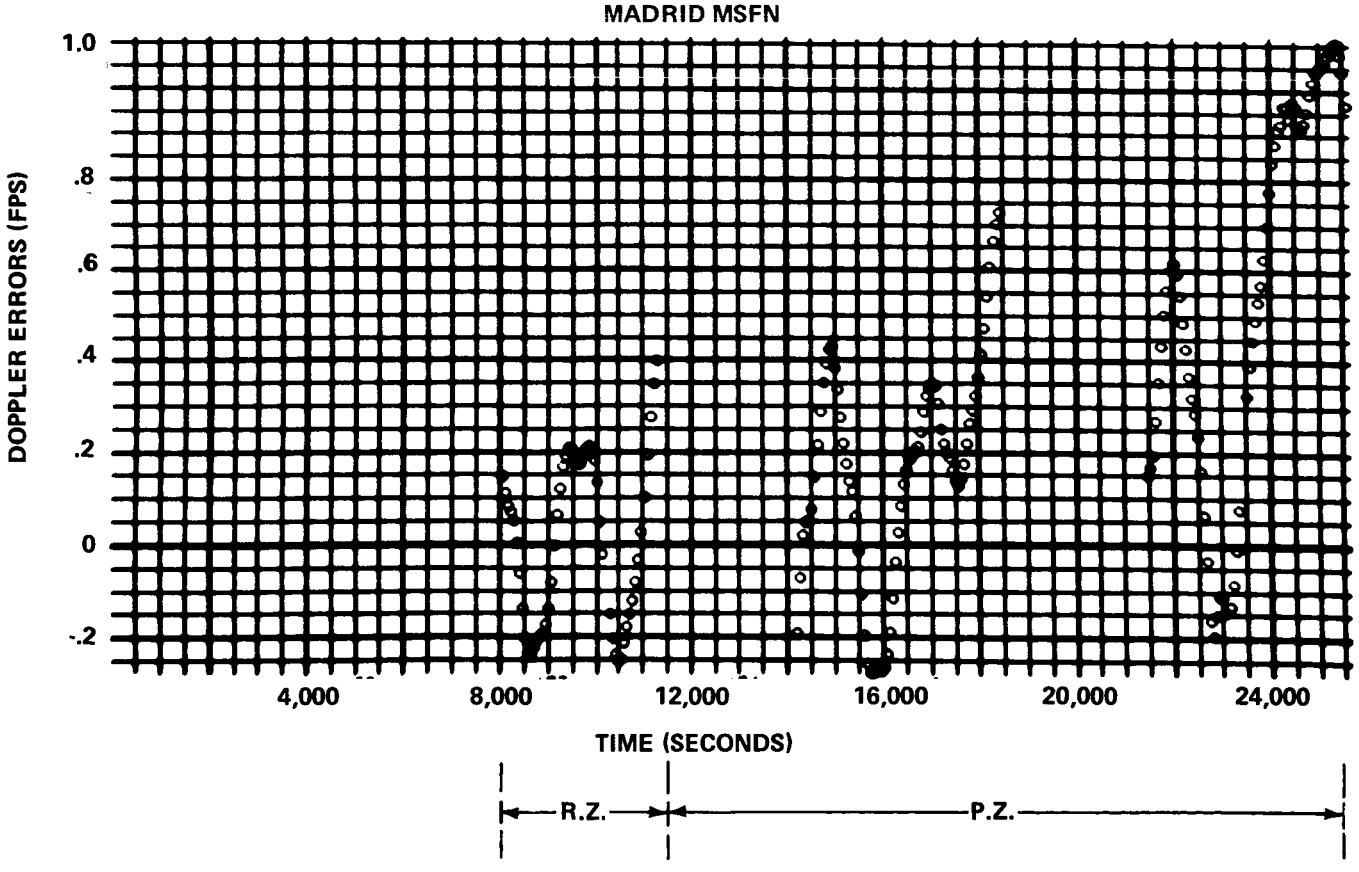

FIGURE 17- PASSES: 19,20 R.Z./ 21,22 P.Z.

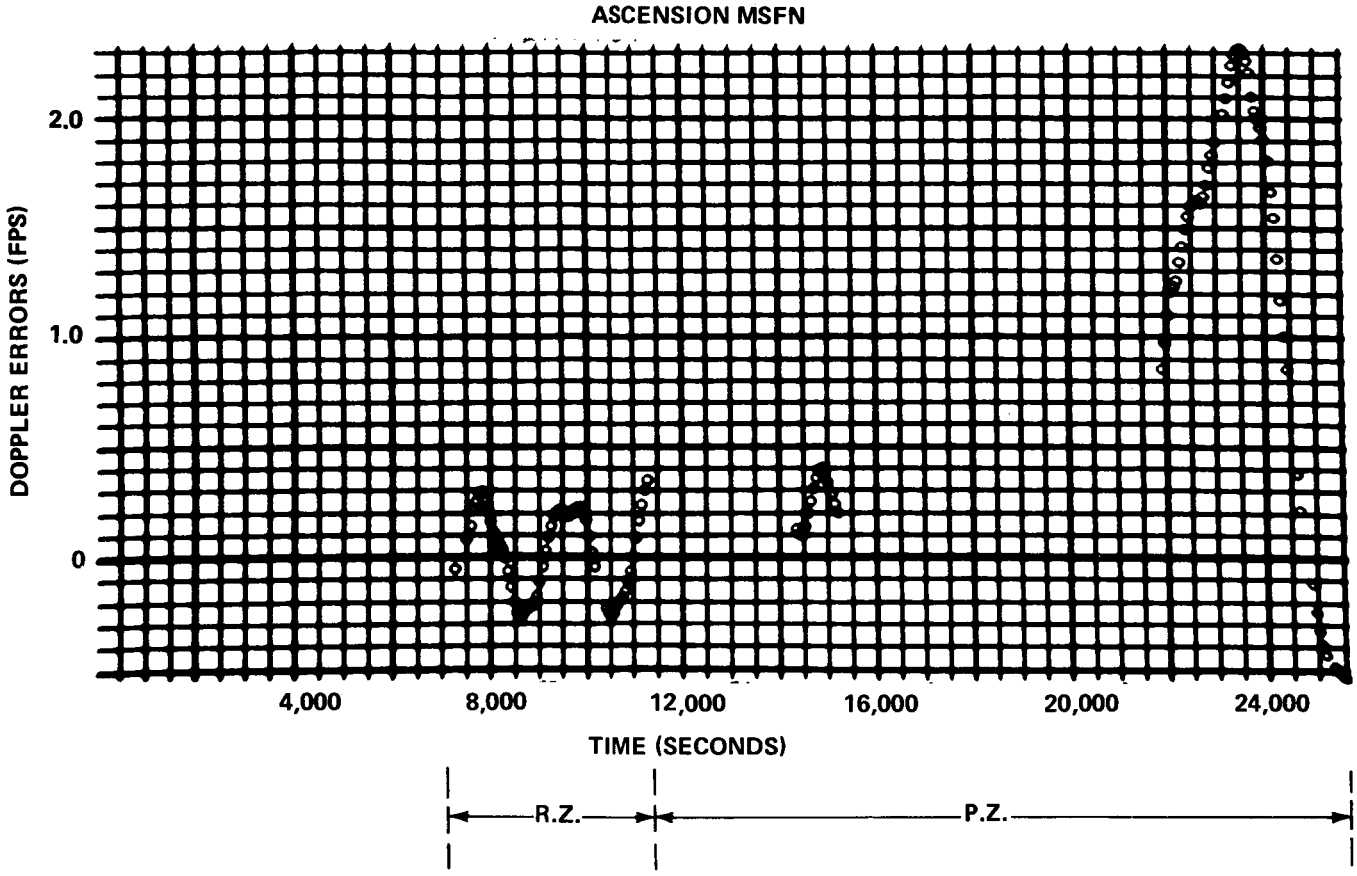

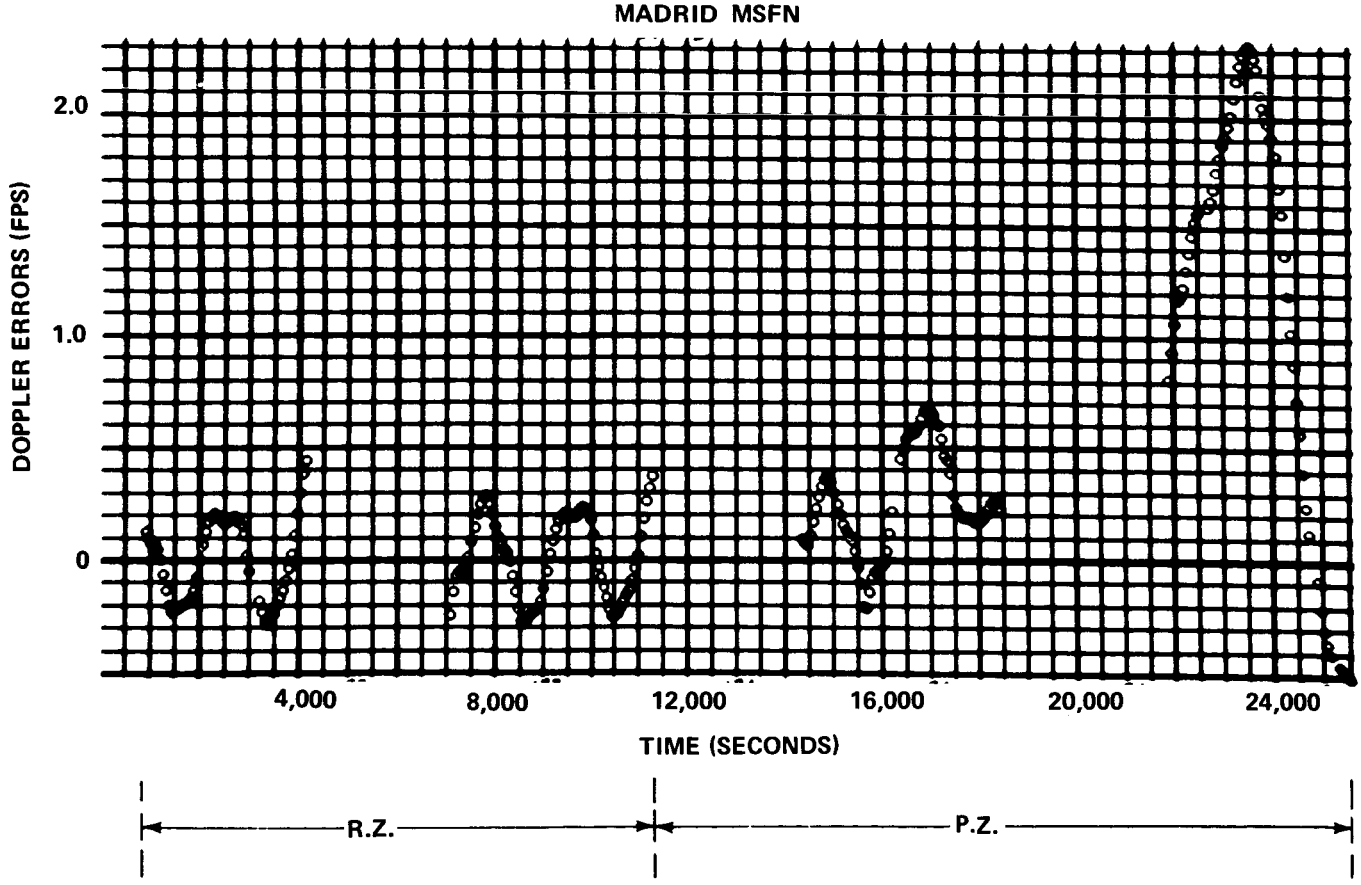

FIGURE 18- PASSES: 20,21 R.Z./22,23 P.Z.

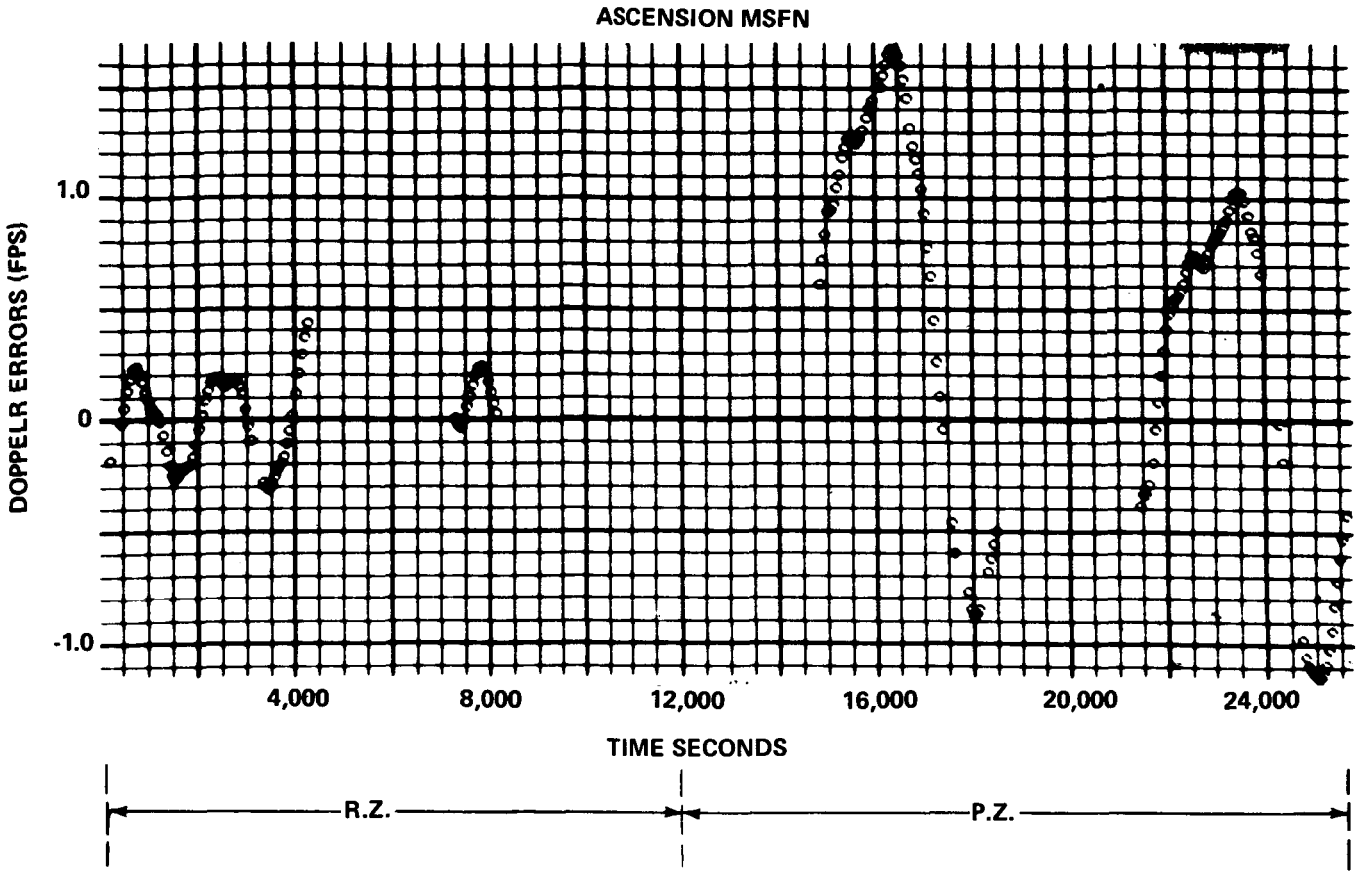

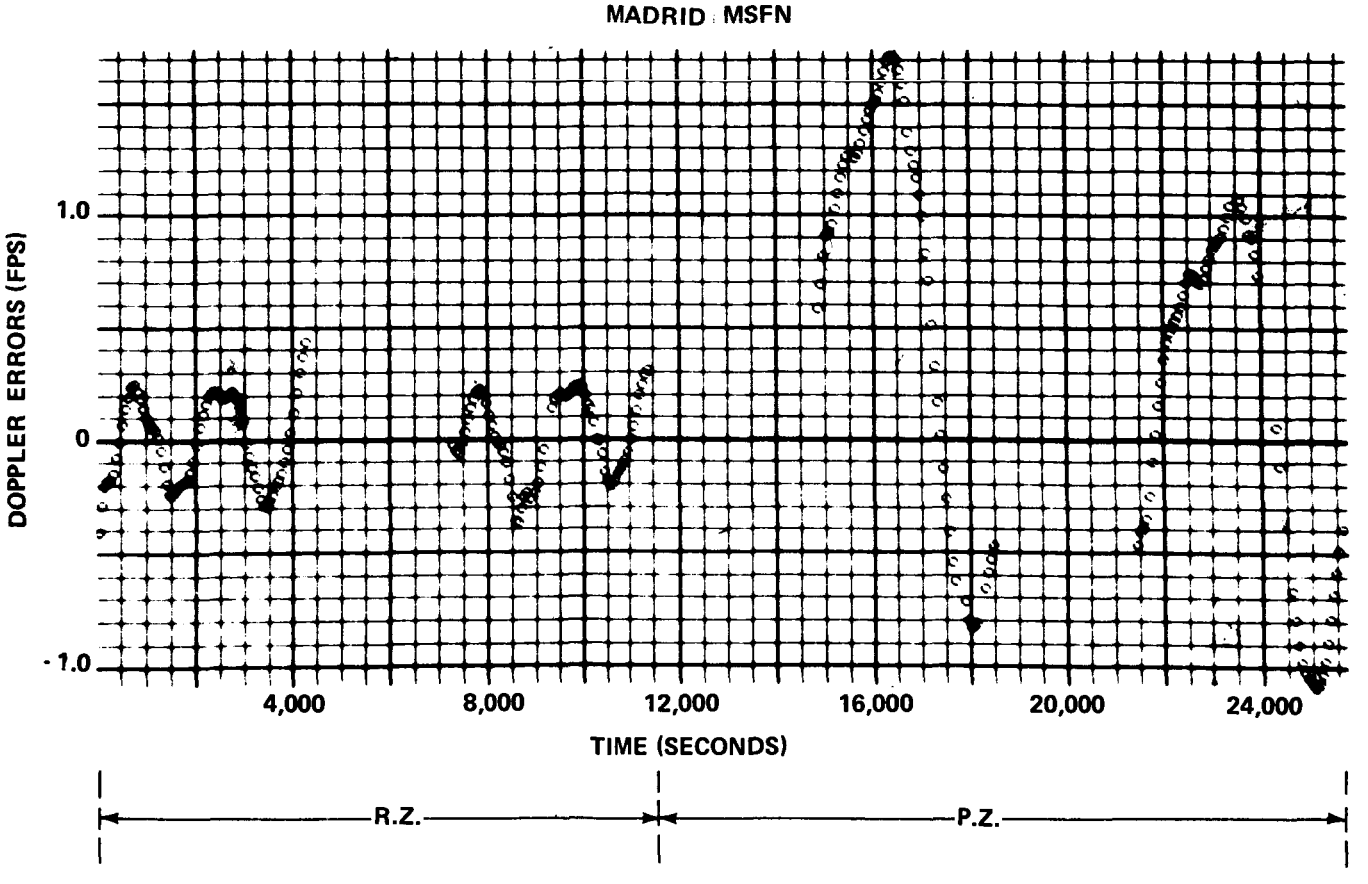

FIGURE 19- PASSES: 21,22R.Z./23,24 P.Z

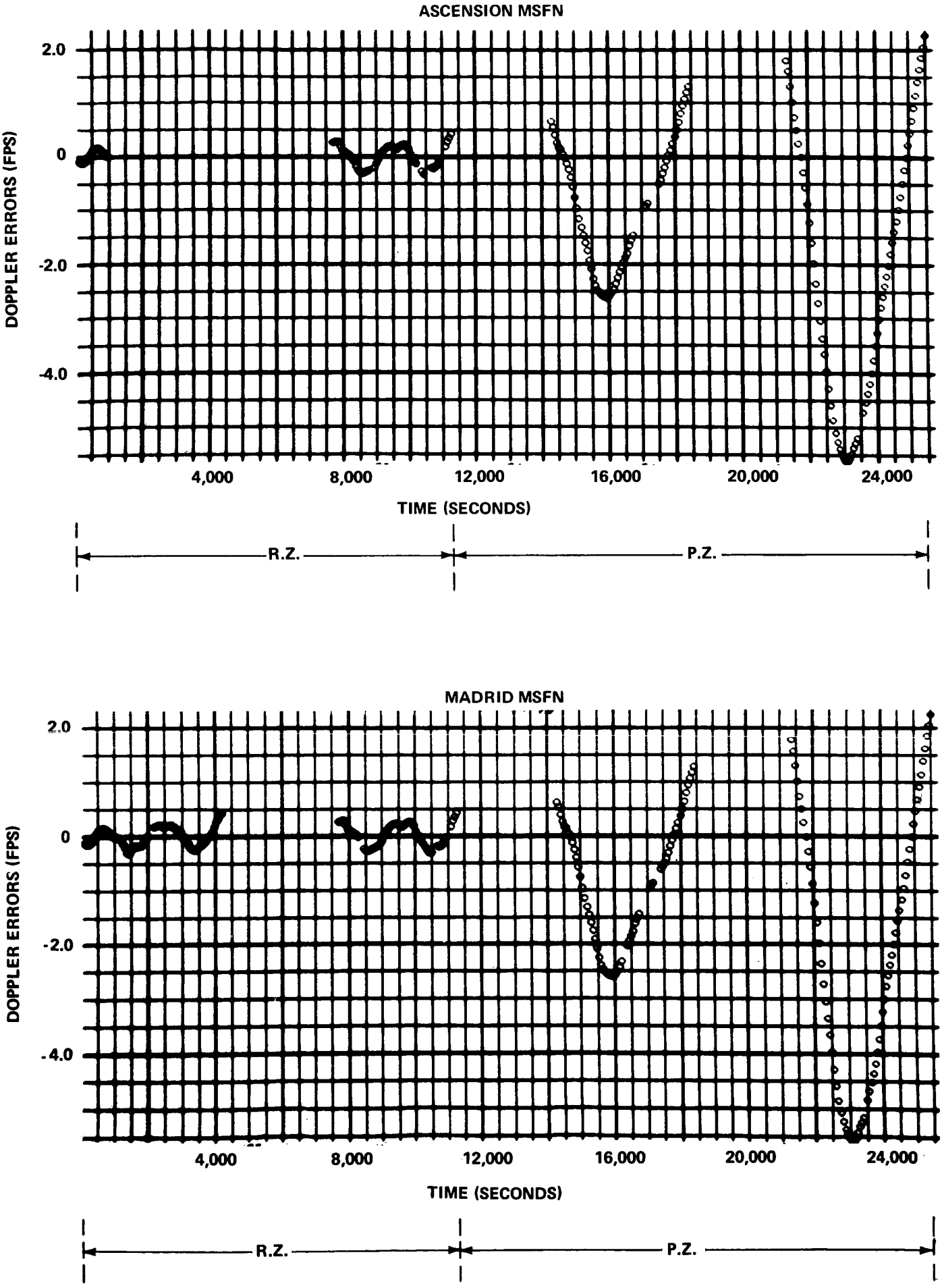

FIGURE 20- PASSES: 22,23 R.Z./24,25 P.Z.

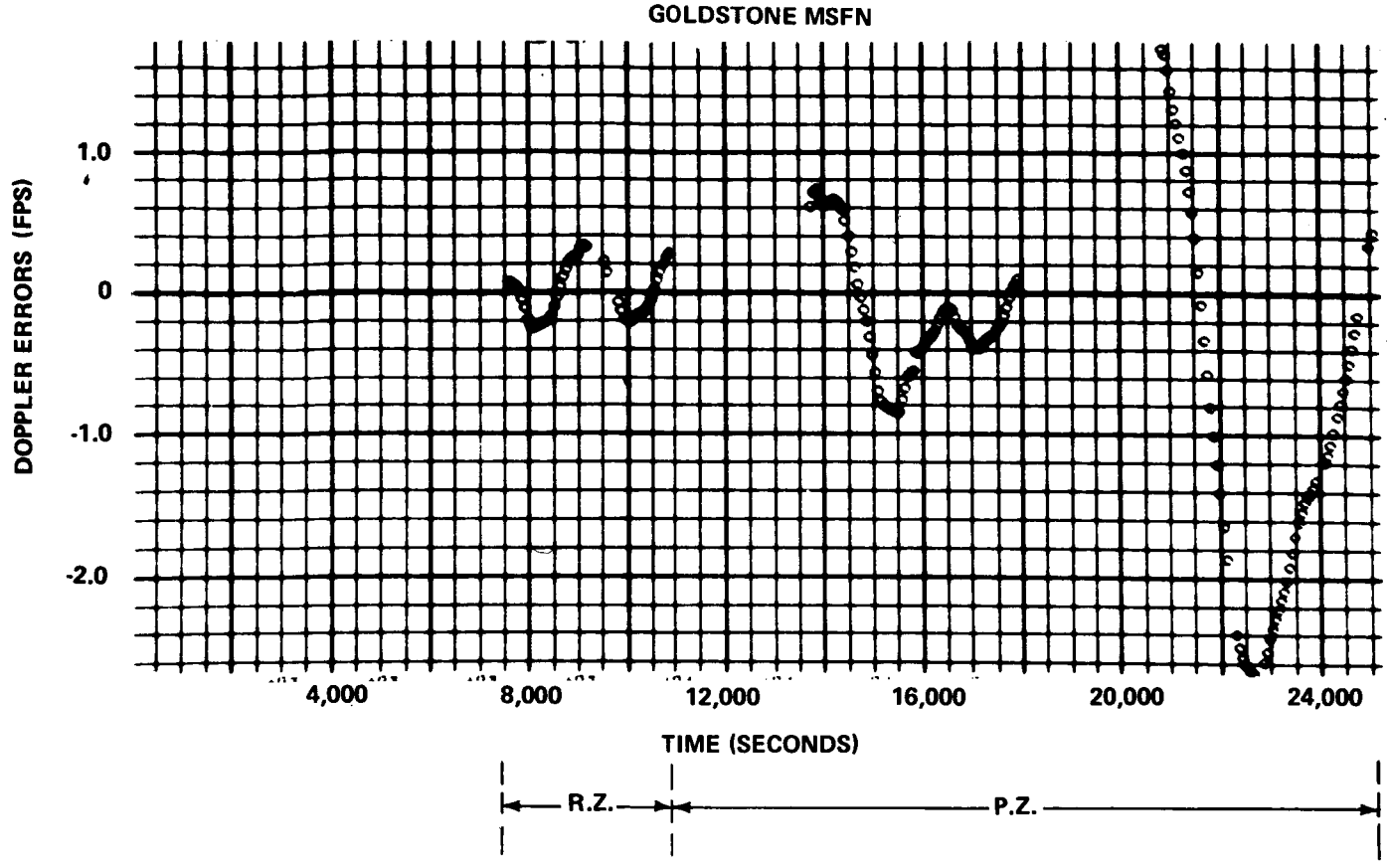

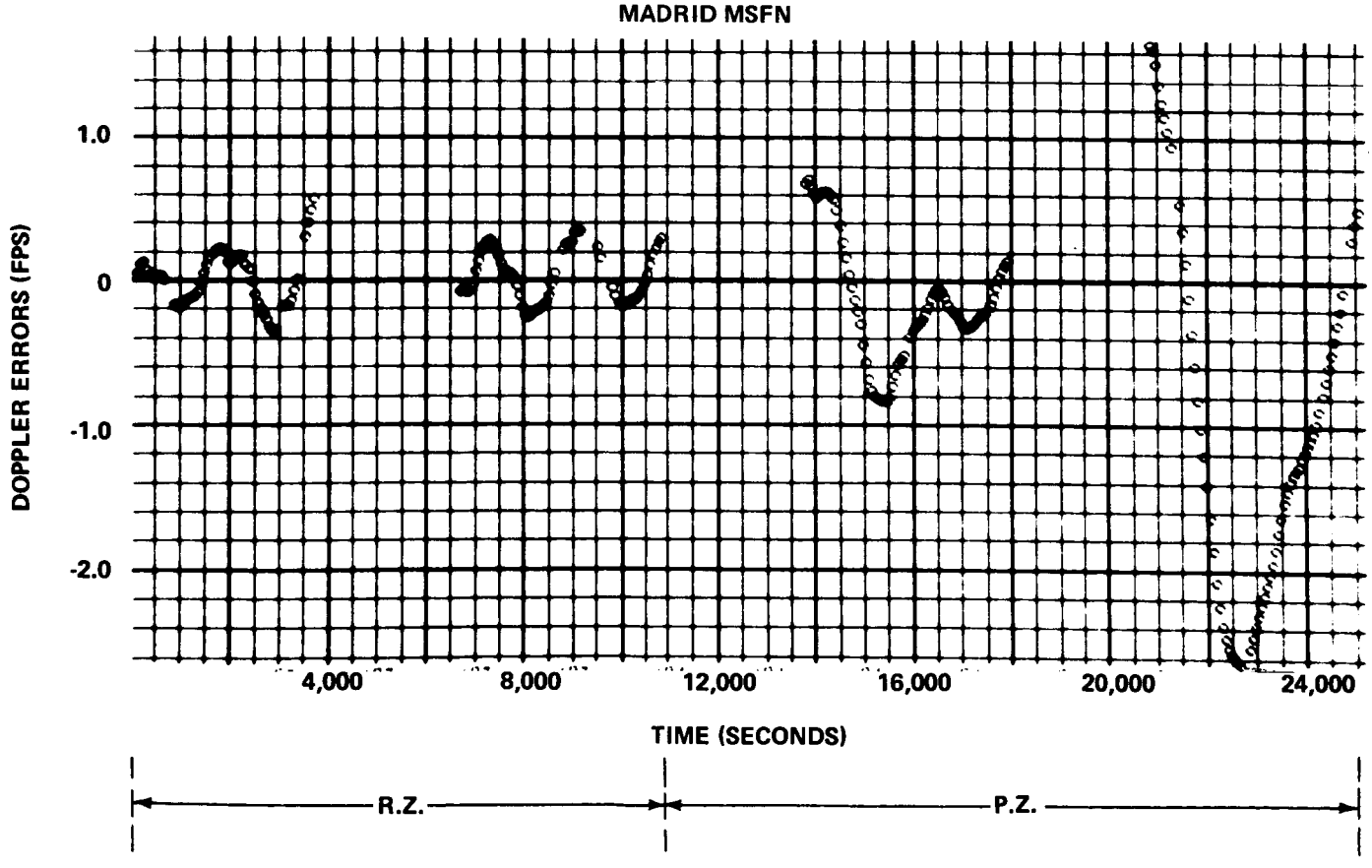

FIGURE 21- PASSES: 23,24 R.Z./ 25,26 P.Z.

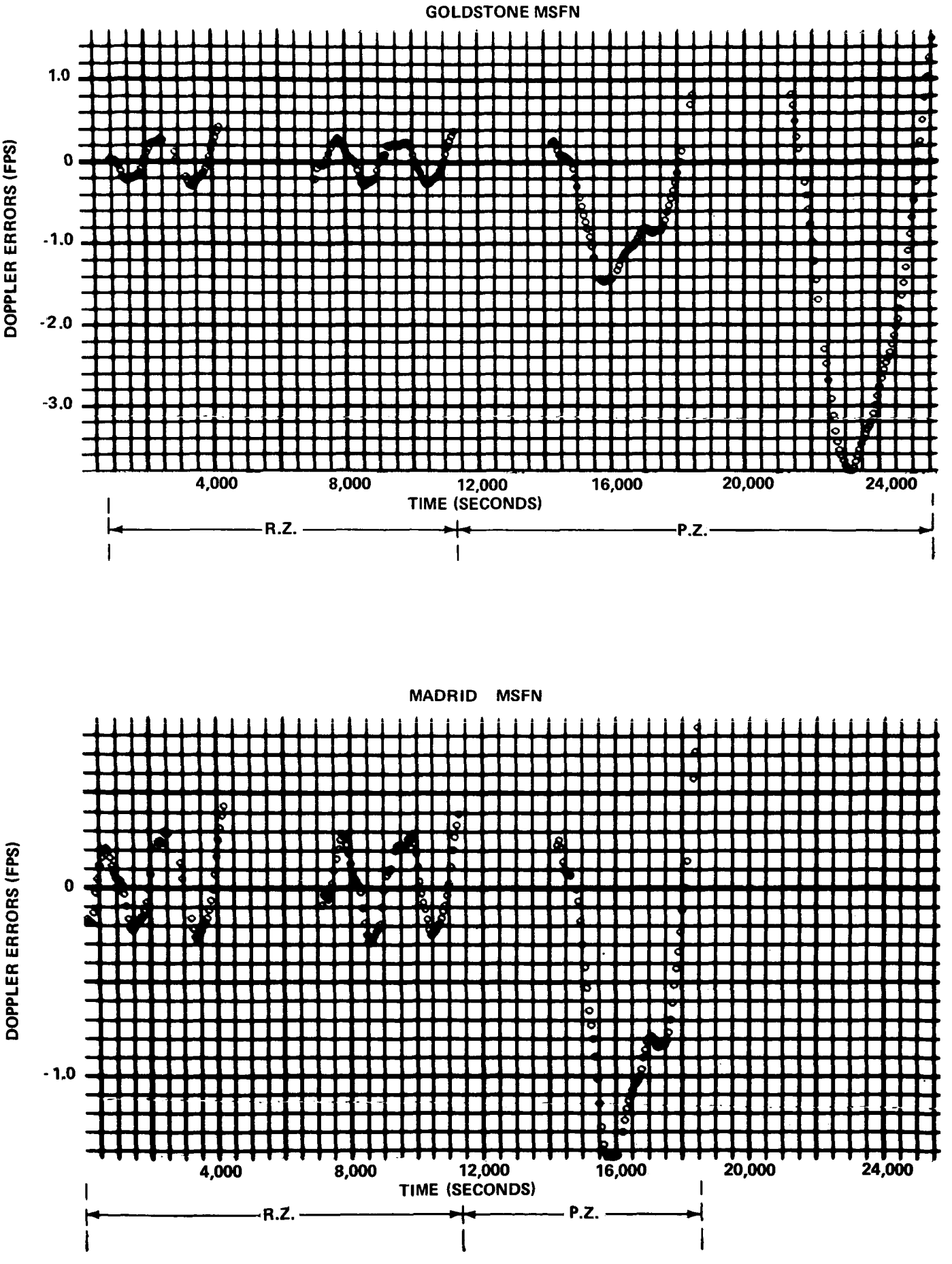

FIGURE 22- PASSES: 24,25 R.Z./26,27 P.Z.